AD NUMBER

ADB232680

NEW LIMITATION CHANGE

TO

Approved for public release, distribution unlimited

FROM

Distribution authorized to U.S. Gov't. agencies only; Proprietary Info.; Jan 98. Other requests shall be referred to Rome Laboratory [OCSM], Rome, NY 13441-4514.

AUTHORITY

AFRL/IFOIP ltr, 15 Jun 2004

RL-TR-97-127
Final Technical Report
October 1997


# TWO-DIMENSIONAL PROCESSING FOR RADAR SYSTEMS

Scientific Studies Corporation

Jaime R. Roman and Dennis W. Davis

Prop. Info. 1-98





Rome Laboratory
Air Force Materiel Command
Rome, New York

RL-TR-97-127 has been reviewed and is approved for publication.

APPROVED: James H. Michels

JAMES H. MICHELS
Project Engineer

FOR THE DIRECTOR: Donald W. Hanson

DONALD W. HANSON, Director
Surveillance & Photonics Directorate

DESTRUCTION NOTICE - For classified documents, follow the procedures in DOD 5200.22M. Industrial Security Manual or DOD 5200.1-R, Information Security Program Regulation. For unclassified limited documents, destroy by any method that will prevent disclosure of contents or reconstruction of the document.

If your address has changed or if you wish to be removed from the Rome Laboratory mailing list, or if the addressee is no longer employed by your organization, please notify Rome Laboratory/OCSM, 26 Electronic Pky, Rome, NY 13441-4514. This will assist us in maintaining a current mailing list.

Do not return copies of this report unless contractual obligations or notices on a specific document require that it be returned.

# REPORT DOCUMENTATION PAGE

*Form Approved*
*OMB No. 0704-0188*



| 1. AGENCY USE ONLY *(Leave blank)* | 2. REPORT DATE | 3. REPORT TYPE AND DATES COVERED | |
|---|---|---|---|
| | October 1997 | Final | Mar 96 - Jan 97 |

**4. TITLE AND SUBTITLE**

TWO-DIMENSIONAL PROCESSING FOR RADAR SYSTEMS

**5. FUNDING NUMBERS**

C - F30602-96-C-0139
PE - 65502F
PR - 3005
TA - 61
WU - 29

**6. AUTHOR(S)**

Jaime R. Roman and Dennis W. Davis

**7. PERFORMING ORGANIZATION NAME(S) AND ADDRESS(ES)**

Scientific Studies Corporation
2250 Quail Ridge Road
Palm Beach Gardens, FL 33418

**8. PERFORMING ORGANIZATION REPORT NUMBER**

N/A

**9. SPONSORING/MONITORING AGENCY NAME(S) AND ADDRESS(ES)**

Rome Laboratory/OCSM
26 Electronic Pky
Rome, NY 13441-4514

**10. SPONSORING/MONITORING AGENCY REPORT NUMBER**

RL-TR-97-127

**11. SUPPLEMENTARY NOTES**

Rome Laboratory Project Engineer: James H. Michels/OCSM/(315) 330-4432

**12a. DISTRIBUTION AVAILABILITY STATEMENT**

Prop. Info

Distribution authorized to U.S. Government agencies only; ~~specific authority: DOD FAR Supplement 252.227-7018~~. Other requests for this document shall be referred to RL/OCSM, Rome, NY. 13441-4514

**12b. DISTRIBUTION CODE**

1-98

**13. ABSTRACT** *(Maximum 200 words)*

Report developed under SBIR Contract. The model-based multichannel detection formulation is presented in the context of a two-dimensional (2-D) representation for space-time processes in general, and airborne surveillance phased array radar systems in particular. For the phased array space-time adaptive processing (STAP) problem, such a formulation requires 2-D parametric models for the channel output process under each one of two mutually exclusive hypotheses. Results presented herein demonstrate the applicability of 2-D model identification algorithms and methods to the phased array STAP problem. Specifically, it is demonstrated that 2-D model identification algorithms provide representative models for airborne surveillance phased array simulated data. Furthermore, the identified models can be used to design hypothesis filters for use in the innovations-based detection methodology resulting from the binary hypothesis testing formulation for moving target detection pioneered by Metford and Haykin (1985) and extended by Michels (1991) to the complex-valued multichannel case. This is a novel feature of the work reported herein.

**14. SUBJECT TERMS**

SBIR Report, Phased Array Radar, Two-Dimensional ARMA Models, Space-Time Adaptive Processing, Model-based Detection, Parametric Modeling, Multichannel Time

**15. NUMBER OF PAGES**

80

**16. PRICE CODE**

| 17. SECURITY CLASSIFICATION OF REPORT | 18. SECURITY CLASSIFICATION OF THIS PAGE | 19. SECURITY CLASSIFICATION OF ABSTRACT | 20. LIMITATION OF ABSTRACT |
|---|---|---|---|
| UNCLASSIFIED | UNCLASSIFIED | UNCLASSIFIED | UL |

## TABLE OF CONTENTS

## LIST OF FIGURES

## LIST OF TABLES

## LIST OF VARIABLES

| | |
|---|---|
| $H_i$ | ith moving target detection problem hypothesis ($i = 0, 1$) |
| A | Whitening filter $n_s x n_s$ system matrix |
| $A(z_d,z_s)$ | Scalar auto-regressive complex-valued 2-D polynomial |
| $B(z_d,z_s)$ | Scalar moving-average complex-valued 2-D polynomial |
| C | Auxiliary matrix |
| D | JxJ diagonal matrix in LDU decomposition of $\Omega$ |
| $E(f_d,f_s)$ | Scalar 2-D equation error function for STAP application |
| $E_m(f_d,f_s)$ | Scalar 2-D equation error function |
| $E_o(z_d,z_s)$ | Scalar 2-D error function |
| F | Innovations representation $n_s x n_s$ system matrix |
| $G_s$ | Number of moving targets (desired signals) |
| $G(f_d,f_s)$ | Scalar 2-D auxiliary function |
| H | Innovations representation $n_s x J$ output matrix |
| I | Identity matrix |
| J | Number of output channels |
| K | Number of independent range cell realizations; $n_s x J$ Kalman gain matrix |
| L | JxJ lower-triangular matrix in LDU decomposition of $\Omega$ |
| M | Number of parameters in an ARMA(P,Q) model |
| N | Number of points in channel output sequence |
| P | Auto-regressive model order |
| Q | Moving-average model order |
| $S_{GI}(f_d,f_s)$ | Generalized innovations model 2-D power spectrum |

| | |
|---|---|
| $S_{GW}(f_d,f_s)$ | Generalized whitening filter 2-D power spectrum |
| $S_{xx}(f_d,f_s)$ | Scalar 2-D power spectrum of $\{x(n,k)\}$ |
| $S_{vv}(f_d,f_s)$ | Generalized innovations 2-D power spectrum |
| T | Innovations spatial whitening and variance normalization JxJ transformation matrix |
| $T_{GI}(z_d)$ | Generalized innovations transfer function matrix |
| $T_{GW}(z_d)$ | Generalized whitening filter transfer function matrix |
| $T_{IR}(z_d)$ | Innovations representation transfer function matrix |
| $T_{WF}(z_d)$ | Whitening filter transfer function matrix |
| $T(z_d,z_s)$ | Scalar 2-D rational transfer function |
| $T_u(z_d,z_s)$ | Scalar unknown 2-D transfer function |
| $U(z_d,z_s)$ | Scalar 2-D input transfer function |
| $X(f_d,f_s)$ | Scalar 2-D frequency domain representation of $x(n,k)$ |
| $X(z_d,z_s)$ | Two-dimensional Z-transform of $x(n,k)$ |
| a(n,k) | (n,k)th AR model parameter |
| b(n,k) | (n,k)th MA model parameter |
| d | Linear array element spacing |
| $\underline{e}_J(f_s)$ | J-element spatial frequency vector |
| $f_d$ | Normalized temporal (Doppler) frequency variable |
| $f_s$ | Normalized spatial frequency variable |
| j | Imaginary unit |
| m | Normalized time lag index variable |
| n | Normalized time index variable |
| $r_{xx}(m,\ell)$ | Scalar 2-D auto-correlation sequence of $\{x(n,k)\}$ |
| $\underline{s}$ | JN-element steering vector |

| | |
|---|---|
| $u(n,k)$ | $(n,k)$th term of white noise scalar 2-D sequence |
| $\underline{w}_o$ | Conventional optimal $JN$-element weight vector |
| $\underline{x}$ | $JN$-element complex-valued data vector |
| $\underline{x}(n)$ | $n$th term of the channel output complex-valued vector sequence |
| $x_i(n)$ | $i$th element of the $n$th term of the channel output complex-valued vector sequence |
| $x(n,k)$ | $(n,k)$th term of the channel output scalar 2-D complex-valued sequence |
| $y(n,k)$ | $(n,k)$th term of scalar 2-D complex-valued ARMA(P,Q) output sequence |
| $z_d$ | Temporal (Doppler) complex-valued variable |
| $z_s$ | Spatial complex-valued variable |
| $N(z_d,z_s)$ | Two-dimensional $Z$-transform of $v(n,k)$ |
| $\Pi$ | Innovations representation $n_s x n_s$ state covariance matrix |
| $\Omega$ | Temporal innovations $JxJ$ covariance matrix |
| $\underline{\alpha}(n)$ | Innovations representation $n_s$-element state vector at time $n$ |
| $\delta(m)$ | One-dimensional Kronecker delta function |
| $\delta(m,\ell)$ | Two-dimensional Kronecker delta function |
| $\underline{\varepsilon}(n)$ | $J$-element temporal innovations vector at time $n$ |
| $\phi$ | Phased array radar azimuth angle from boresight |
| $\gamma$ | Surveillance aircraft crab angle |
| $\eta$ | Conventional optimal joint-domain detection statistic |
| $\kappa$ | Spatial index limit value ($\kappa = J - 1$) |

| | |
|---|---|
| $\lambda_c$ | Narrowband array radiation wavelength |
| $\underline{v}_o$ | JN-element residual vector |
| $\underline{v}(n)$ | Fully-whitened innovations vector sequence |
| $v_i(n)$ | ith element of the nth term of the innovations vector sequence |
| $\underline{v}(n\|H_i)$ | nth term of the residual vector sequence under the ith hypothesis |
| $\theta$ | Phased array radar elevation angle from boresight |
| $\hat{\sigma}_v^2$ | Residual sequence power (variance) estimate |
| $\hat{\mathcal{R}}$ | Estimate of the JNxJN sample covariance matrix |
| $\ell$ | Normalized spatial lag index variable |

## LIST OF MATHEMATICAL SYMBOLS

| | |
|---|---|
| AR(P) | Auto-regressive model of order P |
| ARMA(P,Q) | Auto-regressive moving-average model of order $(P_d,P_s,Q_d,Q_s)$ |
| ARMA(P,Q) | Auto-regressive moving-average model of order (P,Q) |
| MA(Q) | Moving-average model of order Q |
| E[•] | Expectation operator (expected value of •) |
| H | Hermitian transpose operator (as an exponent) |
| T | Transpose operator (as an exponent) |
| Z | Discrete-time transform operator |
| e | Natural logarithm base (e = 2.718281...) |
| $\Sigma$ | Summation operator (with or without specified limits) |
| $\pi$ | 3.141592... |
| -1 | Inverse matrix operator (as an exponent) |
| 1/2 | Square-root operator (as an exponent) |
| -1/2 | Inverse square-root operator (as an exponent) |
| = | "Equal to" |
| $\neq$ | "Not equal to" |
| > | "Greater than" |
| $\geq$ | "Greater than or equal to" |
| < | "Less than" |
| $\leq$ | "Less than or equal to" |
| * | Complex conjugate operator |
| $\Leftrightarrow$ | Two-way association |
| ^ | Estimate |

| | |
|---|---|
| $\forall$ | "For all" |
| $\mid$ | "Such that" |
| $\lvert\bullet\rvert$ | Absolute value of $\bullet$ |
| $\lVert\bullet\rVert$ | Norm of $\bullet$ |
| () | Independent variables of a function |
| {} | Elements of a sequence (or set) |
| ... | Continuation |

## 1.0 INTRODUCTION

This report is a summary of the work carried out by the Scientific Studies Corporation (SSC) team in Phase I of the "Two-Dimensional Processing for Radar Systems" Small Business Innovation Research (SBIR) program for Rome Laboratory (RL). Specifically, the formulations, analyses, and simulation results for space-time processes obtained in the program are presented. The report includes the work carried out by the University of Central Florida (UCF) under contract to SSC.

The model-based multichannel detection formulation is presented in the context of a two-dimensional (2-D) representation for space-time processes in general, and airborne surveillance phased array radar systems in particular. For the phased array space-time adaptive processing (STAP) problem, such a formulation requires 2-D parametric models for the channel output process under each one of two mutually-exclusive hypotheses. Results presented herein demonstrate the applicability of 2-D model identification algorithms and methods to the phased array STAP problem. Specifically, it is demonstrated that 2-D model identification algorithms provide representative models for airborne surveillance phased array radar simulated data. Furthermore, the identified models can be used to design hypothesis filters for use in the innovations-based detection methodology resulting from the binary hypothesis testing formulation for moving target detection pioneered by Metford and Haykin (1985) and extended by Michels (1991) to the complex-valued multichannel case. This is a novel feature of the work reported herein.

The 2-D, least-square, frequency domain (2D-LS-FD) technique formulated by Mikhael and Yu (1994) was adopted in Phase I as the baseline 2-D model identification method. This technique

approximates a given 2-D complex-valued field with a 2-D rational function model of the auto-regressive moving-average (ARMA) class. Of course, the ARMA class includes the auto-regressive (AR) and the moving-average (MA) classes. In this technique the ARMA coefficients are obtained as the solution to a set of linear equations. Excellent results have been obtained in the image noise canceling problem (Mikhael and Yu, 1994), which is related to clutter cancellation in radar space-time processing. This success is duplicated herein for the STAP problem.

The 2D-LS-FD algorithm co-developer, Prof. W. B. Mikhael, Chairman of the Electrical and Computer Engineering Department at UCF, provided support to SSC during Phase I. Dr. Mikhael is a Fellow of the IEEE, and has made extensive contributions in signal and image processing. In Phase I Dr. Mikhael supervised the work of Dr. Q. Z. Zhang, a post-doctoral appointee at UCF with expertise in STAP. Drs. Mikhael and Zhang are both scheduled to continue to provide support in the proposed Phase II.

This report focuses on the phased array STAP problem for airborne surveillance radar systems since such is the main application of interest at RL. However, other contexts are possible, in radar as well as in other applications. As an example, the complex-valued amplitude of the signal collected by a radar system as a function of range and azimuth can be viewed as a 2-D image; the appropriate context for such a case is then space-space processing. Two-dimensional modeling and identification methods can be applied in a wide variety of military, government non-military, and commercial areas. Specifically, such areas include: radar array surveillance systems, active sonar array systems, optical sensor systems, non-destructive inspection (NDI) systems, communication systems, speech processing, medical technology imaging, and geophysical tomography.

An important distinction in the context of radar system applications is that the random processes are represented as complex-valued processes in most cases. Many time series techniques and models have been formulated for complex- as well as real-valued processes. However, the majority of the open-literature results for 2-D algorithms have been established for real-valued processes. This is true in particular for the 2D-LS-FD algorithm selected as the baseline in Phase I. Thus, the 2D-LS-FD algorithm was extended to handle complex-valued processes.

## 1.1 Problem Statement

Consider a linear array radar consisting of J equally-spaced, identical antenna elements (or identical beamformed subarrays) in a side-looking configuration on an airborne surveillance platform moving at a constant speed in level flight. The array is aligned with the aircraft's longitudinal axis, and the aircraft velocity makes a crab angle $\gamma$ with the aircraft's longitudinal axis. The radar array is radiating a coherent pulse train at a constant radiation frequency, and at a constant pulse repetition frequency (PRF). Each antenna element (or group of elements) is referred to as a channel, and the ith channel output (after pulse compression, demodulation, and sampling) corresponding to a single range resolution cell is a complex-valued discrete-time sequence denoted as $\{x_i(n)\}$. The J scalar sequences are concatenated to form a vector sequence $\{\underline{x}(n)\}$. Process $\{\underline{x}(n)\}$ is assumed to be stationary, ergodic, zero-mean, and Gaussian-distributed.

The received signal in an airborne surveillance phased array radar can be referred to as a space-time process, wherein the spatial connotation arises from the spatial diversity of the antenna array elements. In general, the received signal contains a target component, as well as receiver (broadband) noise, jammer noise (broadband interference), and ground clutter (narrowband

interference) components. The one-dimensional (1-D) multichannel (vector) representation of the radar space-time signal has been adopted extensively in the development and analysis of optimum joint-domain adaptive algorithms and sub-optimum block-covariance algorithms for STAP, which encompasses target detection and interference rejection in airborne surveillance radar arrays (Brennan and Reed [1973]; Jaffer et al. [1991]; Ward [1994]). These algorithms are often referred to as the conventional (or classical) STAP algorithms. More recently, Michels (1991) and Román and Davis (1993a; 1993b) have adopted the 1-D vector representation for the development of multichannel AR and state-space models, respectively, for joint-domain innovations-based detection algorithms. Alternatively, a space-time signal can be represented as a 2-D scalar process. The 2-D representation is essential for visualizing and understanding the spectral energy and correlation characteristics of the total signal, and of the ground clutter component in particular. This representation also offers algorithmic and modeling advantages.

With respect to model-based detection for the airborne surveillance phased array radar STAP problem, 1-D models offer dynamic and static degrees of freedom in the temporal axis, but only static degrees of freedom in the spatial axis (see Sections A.2 and A.4). In contrast, 2-D models offer dynamic and static degrees of freedom in both axes (space and time). Thus, a model-based detection methodology using 2-D scalar models is inherently better-suited to the cases wherein channel-to-channel correlation exhibits a complicated structure. Such cases occur physically when the platform and scenario parameters lead to a non-integer-valued clutter ridge slope parameter, to non-zero misalignment between the array longitudinal axis and the platform velocity vector, and to non-zero internal clutter motion. These conditions are common in airborne surveillance radar scenarios.

## 1.2 Report Overview

Model-based multichannel detection in the context of the 2-D representation of the channel output vector process is discussed in Section 2.0, including a summary of 2-D time series models. The 2D-LS-FD model identification method and its formulation for STAP are discussed in Section 3.0. The airborne surveillance phased array radar application is discussed in Section 4.0, including simulation-based results generated using the SSC-developed radar data generation software described in Vol. II of (Román and Davis, 1997). A summary and suggestions for further work are presented in Section 5.0. Appendix A presents a 2-D representation for 1-D vector state-space models, which allows comparison of results obtained using state-space model identification algorithms (Román and Davis, 1997) with those obtained using the 2D-LS-FD algorithm.

## 2.0 MODEL-BASED MULTICHANNEL DETECTION

The model-based approach to multichannel detection involves the generation of an analytic model for the multichannel system, utilization of such model to process the multichannel data, and determination of a detection decision by applying a detection rule to the processed data. A model class is selected to represent the multichannel system, and the model parameter values determine the specific system model. Model parameters can be identified on-line, by applying an identification algorithm to the received channel data. Alternatively, model parameters can be identified off-line for various conditions and stored in the processor memory to be accessed in real-time as required.

For the work reported herein the time series class of 2-D, linear, shift-invariant parametric models is selected. This class includes MA, AR, and ARMA models. Emphasis is placed on the ARMA model subclass because it is more general than the MA and AR subclasses. One-dimensional, vector (multichannel) models have been applied to the multichannel detection problem by Michels (1991) and Román and Davis (1993a; 1993b), and the success obtained in their work provided motivation for this research. Utilization of the 2-D model class in the context of multichannel detection, however, is the most important and novel aspect of the work reported herein.

Two types of 2-D model parameter estimation algorithms can be defined: (a) algorithms which operate on the channel output correlation sequence, and (b) algorithms which operate on the channel output data directly, without calculating correlation information. The AR model identification algorithms discussed by Therrien (1986) are examples of the former, and the 2D-LS-FD algorithm formulated by Mikhael and Yu (1994) is an example of the latter. The 2D-LS-FD is the algorithm selected for this program.

As the name implies, this algorithm is based on the least-square philosophy, in contrast to the stochastic philosophy prevalent in most of the model identification literature.

## 2.1 Multichannel Detection

Detection problems in the context of radar systems (as well as in other applications) can be postulated as a binary hypothesis testing problem. Specifically, the class of problems addressed in this report involve the following two hypotheses:

$\mathbf{H}_0$: Target (desired signal component) is absent

$\mathbf{H}_1$: Target (desired signal component) is present

$\mathbf{H}_0$ is referred to as the null hypothesis, and $\mathbf{H}_1$ is the alternative hypothesis. The model-based approach to detection with phased array radars is couched on the assumption that the process at the array output can be described by a linear parametric model under each of the two hypotheses, and that the parametric models that correspond to the two hypotheses are sufficiently different to allow selection of the correct hypothesis by the evaluation of measures that are sensitive to those differences. In innovations-based detection, as formulated by Medford and Haykin (1985), Michels (1991), and others, two parallel paths are established for processing the received radar signal. This is illustrated in Figure 2-1 for a general case with off-line parameter estimation. In the top path the received radar sequence, $\{\underline{x}(n)\}$, is processed with a filter tuned to whiten the sequence when $\mathbf{H}_0$ is true, and in the bottom path the received radar sequence is processed with a filter tuned to whiten the sequence when $\mathbf{H}_1$ is true. The filter outputs, $\{\underline{v}(n|\mathbf{H}_i) \mid i = 0, 1; n = 0, 1, \ldots, N\text{-}1\}$, are labeled as residuals; these residuals are true innovations processes when the data condition (hypothesis) matches the filter type. This architecture

is referred to herein as the multichannel innovations-based detection algorithm (MIBDA).

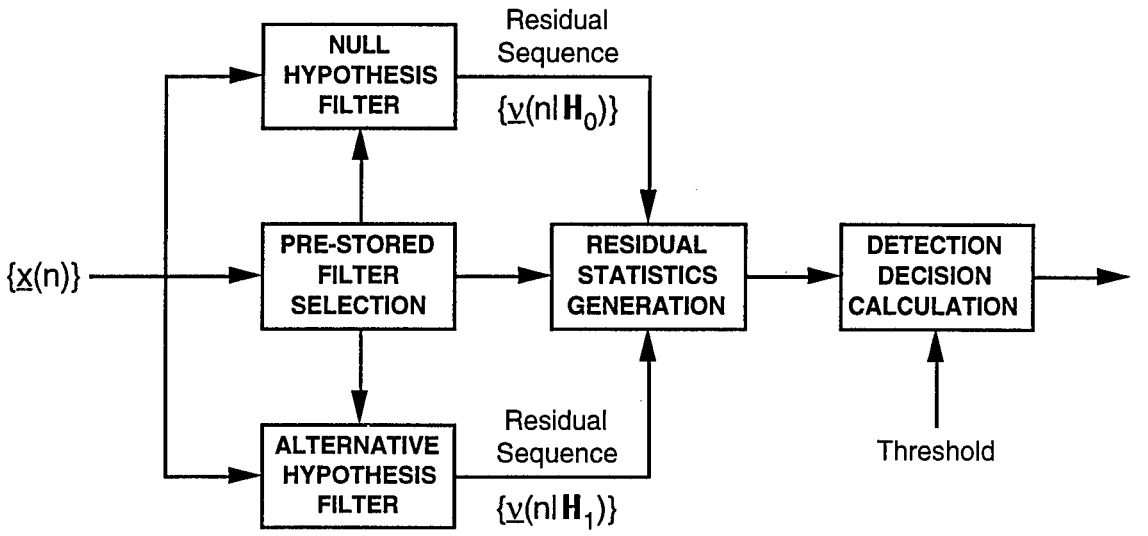


*Figure 2-1. Multichannel innovations-based detection architecture with off-line hypothesis filter design.*

An alternative to the MIBDA detection approach is the model-based or parametric adaptive matched filter (PAMF) formulated by Rangaswamy and Michels (1997). In essence, the PAMF consists of the null hypothesis filter path in Figure 2-1. Of course, the detection statistic and decision rule are modified appropriately.

## 2.2 Scalar, Two-Dimensional Representation of the Channel Output Sequence

The channel output vector sequence $\{\underline{x}(n)\}$ can be viewed as a scalar 2-D sequence (Dudgeon and Mersereau, 1984). Let channel J be the temporal and spatial reference for the array, and define the following association,

(2-1) $x_{J-k}(n) = x(n,k)$ $0 \le n \le N-1;\ 0 \le k \le J-1$

The process $\{x(n,k)\}$ has a scalar 2-D power spectrum denoted as $\{S_{xx}(f_d,f_s)\}$, and a scalar 2-D auto-covariance sequence (ACS) denoted as $\{r_{xx}(m,\ell)\}$, where $(m,\ell)$ is the lag pair corresponding to the frequency pair $(f_d,f_s)$.

The association defined by Equation (2-1) is illustrated in Figure 2-2; this association was adopted herein because it is consistent with the relation between multichannel 1-D and scalar 2-D systems demonstrated by Therrien (1981). Alternatives to Equation (2-1) can be defined, such as $\{x_{k+1}(n) = x(n,k) \mid n = 0, 1, \ldots, N-1; k = 0, 1, \ldots, J-1\}$. This alternative definition corresponds to the MATLAB software default array definition convention.

A block diagram equivalent to that of Figure 2-1 can be defined using the scalar 2-D process $\{x(n,k)\}$ as its input (see Section 3.3). In such a diagram the functionality of the blocks remains the same, but the specific content of each block must accommodate the differences in model class and implementation aspects.

As stated earlier, the time series subclass of 2-D, linear, shift-invariant parametric models was selected to represent the channel output under each of the two hypotheses. The work in Phase I addressed two important issues beyond the work of Michels (1991). First, the channel output is represented as a 2-D scalar random process, with the attendant increase in modeling degrees-of-freedom (independent dynamic and static modeling capability along each axis). Second, the complete time series model class (MA, AR, and ARMA models) was considered, with emphasis on ARMA models due to their higher degree of modeling capacity.

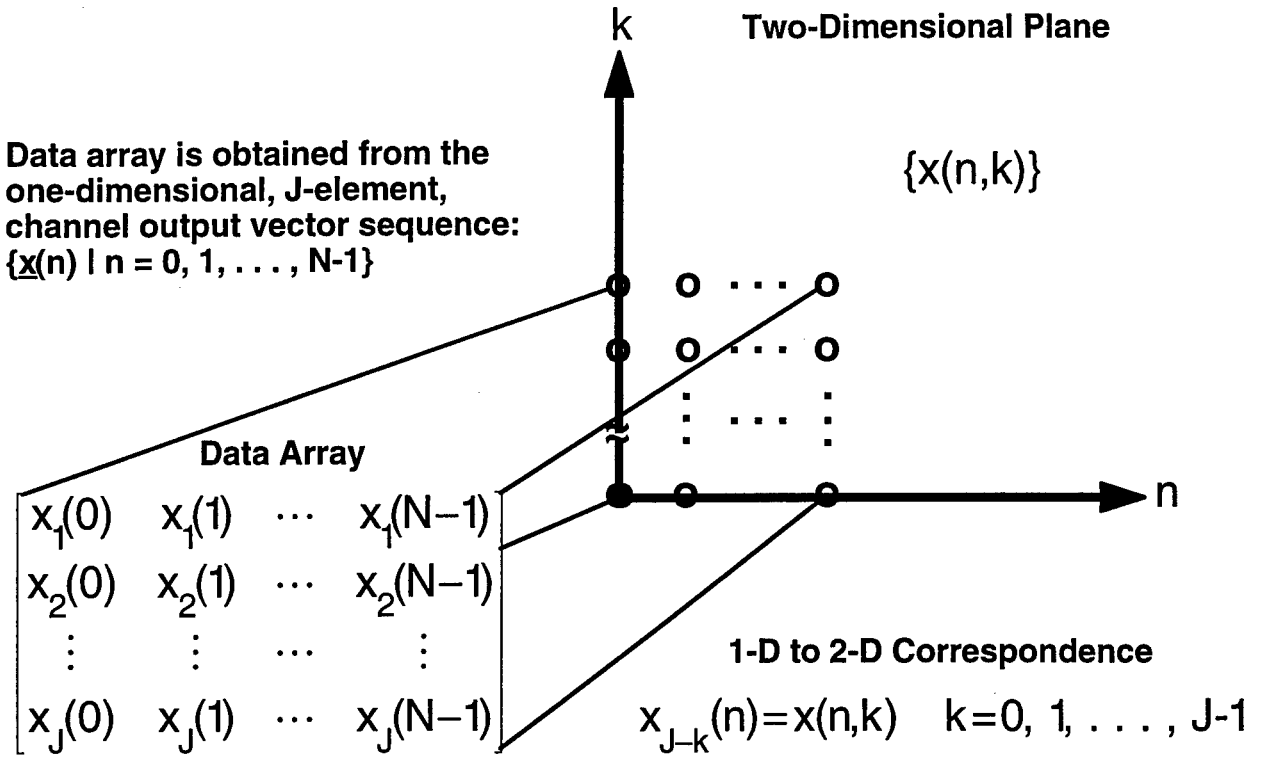


*Figure 2-2. One-D and two-D channel output data representations.*

## 2.3 Two-Dimensional Time Series Models

Model-based detection as considered herein is predicated on the representation of the channel output process {x(n,k)} as the output of a 2-D time series model driven by white noise. Furthermore, the time series model output is corrupted by additive white noise. To be precise, such a representation is approximate in the case of radar data. Nevertheless, in practice time series models have been shown to provide a good fit to radar data; this point is underscored for 2-D models by the results in Section 4.0.

As stated previously, the 2-D process {x(n,k)} is assumed to be represented as

(2-2) $$x(n,k) = y(n,k) + w(n,k)$$

where $y(n,k)$ is the output of a linear, shift-invariant, 2-D time series model, and $w(n,k)$ is a 2-D, zero-mean, Gaussian-distributed, white noise process. The processes $\{y(n,k)\}$ and $\{w(n,k)\}$ are independent.

A 2-D ARMA(P,Q) process $\{y(n,k)\}$ is defined as

(2-3) $$y(n,k) = -\sum_{i_d=1}^{P}\sum_{i_s=1}^{P} a(i_d,i_s)\, y(n-i_d,k-i_s) + \sum_{i_d=0}^{Q}\sum_{i_s=0}^{Q} b(i_d,i_s)\, u(n-i_d,k-i_s)$$

where the input $\{u(n,k)\}$ is a 2-D, zero-mean, Gaussian-distributed, white noise process, and $\{a(i_d,i_s)\}$ and $\{b(i_d,i_s)\}$ are complex-valued, constant coefficients referred to as the AR and the MA parameters, respectively. When $P = 0$ Equation (2-3) is an MA(Q) process, whereas when $Q = 0$ Equation (2-3) is an AR(P) process. The transfer function associated with model (2-3) is obtained as the 2-D Z-transform of Equation (2-3). That is, the transfer function is a 2-D, complex-valued, rational function of the form

(2-4) $$T(z_d,z_s) = \frac{B(z_d,z_s)}{A(z_d,z_s)} = \frac{\sum_{q_d=0}^{Q}\sum_{q_s=0}^{Q} b(q_d,q_s) z_d^{-q_d} z_s^{-q_s}}{\sum_{p_d=0}^{P}\sum_{p_s=0}^{P} a(p_d,p_s) z_d^{-p_d} z_s^{-p_s}}$$

(2-5) $$a(0,0) = 1$$

with complex-valued variables $z_d$ and $z_s$, and where $A(z_d,z_s)$ and $B(z_d,z_s)$ are the AR and MA scalar, 2-D polynomials, respectively. As indicated in Equation (2-5), the leading coefficient of $A(z_d,z_s)$ is unity. This follows from Equation (2-3), and is the 2-D version of a monic polynomial in 1-D. And the 2-D frequency

response of model (2-3), which is denoted as $T(f_d, f_s)$, is obtained by restricting the complex variables $z_d$ and $z_s$ to the unit surface,

(2-6) $$z_d = e^{j2\pi f_d}$$

(2-7) $$z_s = e^{j2\pi f_s}$$

with $f_d$ and $f_s$ the normalized temporal (Doppler) and spatial frequencies, respectively.

In the context of MIBDA processing for surveillance phased array radar systems, modeling involves determination of the parameters $\{a(i_d,i_s)\}$ and $\{b(i_d,i_s)\}$ to represent a moving target, jamming interference, and ground clutter. These channel output components must be modeled either individually, or in any one of the possible combinations, as dictated by the scenario conditions and the processor architecture. For PAMF processing only ground clutter and/or jamming interference must be modeled. In Phase I, emphasis was placed in modeling ground clutter since it drives the requirements for a 2-D model. Having identified the model parameters which represent the process, the associated 2-D whitening (inverse) filter is available directly. Specifically, given the channel output 2-D sequence, $\{x(n,k)\}$, the whitening filter residual sequence, $\{v(n,k)\}$, is obtained as

(2-8) $$v(n,k) = -\sum_{i_d=1}^{Q}\sum_{i_s=1}^{Q} b(i_d,i_s)\, v(n-i_d,k-i_s) + \sum_{i_d=0}^{P}\sum_{i_s=0}^{P} a(i_d,i_s)\, x(n-i_d,k-i_s)$$

If model (2-2)-(2-3) represents the channel output exactly and the noise $\{w(n,k)\}$ is zero, then $\{v(n,k)\}$ is a true innovations sequence. For any other conditions, the filter residual approximates an innovations. Notice that the whitening filter is also an ARMA system, but with the roles of the AR and MA coefficients reversed.

A 2-D model of the form in Equation (2-3) is referred to as a first-quadrant system since only values in the first quadrant of the input and output 2-D planes (except for initial conditions) are used to generate the system output. Model (2-3) is causal, in loose analogy with the 1-D case, since only past outputs and present and past inputs are used to generate the present output. In the phased array radar space-time problem causality along the time axis is an inherent feature of the channel output. In contrast, the issue of causality along the spatial axis is not clear because all channels generate an output at each temporal sampling instant. Model (2-3) is also recursively computable (Dudgeon and Mersereau, 1984), which simplifies hardware implementation. Other region of support options, such as the non-symmetric half plane (NSHP), are of interest and will be considered in Phase II.

Two-dimensional time series models have several features quite distinct from their 1-D counterparts. To begin, 2-D models offer more dynamic as well as static modeling degrees-of-freedom. On the negative side, most 2-D polynomials are not factorable. Thus, polynomials $A(z_d, z_s)$ and $B(z_d, z_s)$ identified by an algorithm are likely to be unfactorizable. This complicates key issues such as stability determination. In 2-D systems, poles and zeros can occur as functions rather than as an isolated point (Dudgeon and Mersereau, 1984). Also, causality and region of support issues often present a variety of alternatives, in contrast with single options in 1-D systems. All cases considered in Phase I resulted in a stable 2-D model.

Estimation of the parameters for the 2-D scalar time series models has been addressed by several authors (see [Marple, 1987], [Dudgeon and Mersereau, 1984], [Therrien, 1986] and the references therein). For AR models most algorithms require generation of the ACS of the process, and the algorithms are extensions of the 1-D

case. In contrast with the 1-D case, for 2-D systems the maximum entropy method (MEM) is not equivalent to the AR method. Further, the MEM parameters are obtained via optimization procedures, with their attendant convergence and other such difficulties. Most 2-D model identification algorithms are formulated in a stochastic framework and require the ACS (in practice, only an estimate of the ACS is available). An exception is the 2D-LS-FD method developed recently by Mikhael and Yu (1994). The 2D-LS-FD algorithm is a least-square method, as its name implies, and is the algorithm selected in Phase I.

A generalized version of the 2-D ARMA(P,Q) process can be defined by allowing distinct values for the model order along each dimension. Specifically, a 2-D ARMA($\underline{P}$,$\underline{Q}$) process {y(n,k)} is defined as

$$(2\text{-}9) \qquad y(n,k) = -\sum_{i_d=1}^{P_d}\sum_{i_s=1}^{P_s} a(i_d,i_s)\, y(n-i_d,k-i_s) + \sum_{i_d=0}^{Q_d}\sum_{i_s=0}^{Q_s} b(i_d,i_s)\, u(n-i_d,k-i_s)$$

where the input process and system parameters are as defined previously, and $\underline{P} = [P_d,P_s]$, $\underline{Q} = [Q_d,Q_s]$. The transfer function and residual for model (2-9) follow trivially. A system of the form (2-9) is a more relevant model for the STAP application because the data duration along the temporal axis is usually longer than the data duration along the spatial axis (the data matrix is rectangular).

## 3.0 TWO-DIMENSIONAL, LEAST-SQUARE, FREQUENCY-DOMAIN (2D-LS-FD) ALGORITHM FOR MIBDA PROCESSING

The 2D-LS-FD method is based on a modification to the output error model method, and is an extension of prior work for the 1-D case. The output error model method is a model matching approach, which inherently invokes least-squares optimization. Such a formulation is in contrast with the stochastic formulation common to most model identification algorithms. The method can be viewed also as a direct approach, since the algorithm operates on the channel output data directly, without the requirement to estimate the channel output ACS. A key feature of the 2D-LS-FD method is that the parameters of the 2-D polynomial model are calculated by solving a linear set of equations in the frequency domain. Another important feature of the 2D-LS-FD method is that an indication of model order is available by the dimension of a subspace, which translates into verifying the rank of a matrix. Additionally, the 2D-LS-FD method admits alternative algorithmic variations, which provides a wealth of possible approaches to model the airborne surveillance phased array radar return. Due to these features, the 2D-LS-FD method was the baseline algorithm for Phase I.

Originally, the 2D-LS-FD method was developed for real-valued data, and for a square ARMA model, Equation (2-3), since these are the conditions that apply in image processing applications such as data compression and noise cancellation. In Phase I the method was extended to handle the complex-valued case and the rectangular ARMA model, Equation (2-9). Both extensions turned out to be straightforward. The main issue in the extension to complex-valued data is to insure that the rules of complex-valued operations (inner product; 2-norm; etc.) are satisfied. A MATLAB-based software implementation of a fast algorithm was developed also in Phase I.

A MATLAB set of routines was generated to model the complex-valued version of the 2D-LS-FD algorithm. These routines were tested and validated using several test cases, including an ARMA(1,1) system, and a signal with a power spectrum consisting of the sum of three Gaussian-shaped peaks. Once the software was validated, it was exercised to model and to whiten simulated airborne surveillance phased array radar data generated with the SSC-generated simulation for a variety of system parameter values and scenario conditions. The SSC simulation is described in Vol. II of the report by Román and Davis (1997).

Model order determination is a fundamental issue for all model identification algorithms, including the 2D-LS-FD method. The approach postulated by SSC and pursued in Phase I is based on the characteristics of the residual generated using the inverse (whitening) system of the identified model.

### 3.1 2D-LS-FD Method for 2-D Model Identification

Consider the output error model configuration defined in Figure 3-1, which is presented in 2-D $Z$-transform domain (all functions are complex-valued). In Figure 3-1, the 2-D function $T_u(z_d,z_s)$ represents an unknown system, $T(z_d,z_s)$ represents an ARMA model (2-9), $U(z_d,z_s)$ is the 2-D driving white noise function, and $E_o(z_d,z_s)$ is the 2-D error function. It is important to recognize that the unknown system is unrestricted (that is, it can be different from an ARMA). In equation form, the output error is

$$E_o(z_d,z_s) = U(z_d,z_s)\,[T_u(z_d,z_s) - T(z_d,z_s)] \tag{3-1}$$

and the 2-norm of the output error restricted to the unit surface (Equations (2-6) and (2-7)) is defined as

$$(3\text{-}2) \qquad \left\| E_o(f_d, f_s) \right\|_2 = \left[ \int_{-0.5}^{0.5} \int_{-0.5}^{0.5} \left| E_o(f_d, f_s) \right|^2 df_d \, df_s \right]^{1/2}$$

Minimization of the 2-norm in Equation (3-2) with respect to the ARMA model parameters generates a model which is an optimum approximation to the unknown system for the selected model order. The function $U(f_d,f_s)$ serves as a weighting term; as such, Equation (3-2) represents a weighted 2-norm minimization.

Most methods available for minimizing (3-2) are nonlinear, which presents computational problems and convergence issues. Recently, however, Mikhael and Yu (1994) have developed a formulation which leads to a linear method. Their formulation is based on the variation of Figure 3-1 shown in Figure 3-2 for the case of an ARMA model, and is referred to as the equation error model method. In this report the equation error is denoted with subscript "m" in order to emphasize the difference between the two formulations. Notice that all 2-D functions in Figure 3-2 are restricted to the unit surface in the frequency domain. In equation form, the equation error of Figure 3-2 is

$$(3\text{-}3) \qquad E_m(f_d,f_s) = U(f_d,f_s) \left[ T_u(f_d,f_s) \, A(f_d,f_s) - B(f_d,f_s) \right]$$

Minimization of the 2-norm of the equation error $E_m(f_d,f_s)$ leads to a linear set of equations in the unknown parameters $\{a(i_d,i_s)\}$ and $\{b(i_d,i_s)\}$. The linear set of equations has a solution provided the number of equations is more than or equal to the number of unknown parameters, and provided that the parameter set is constrained appropriately. In this modified formulation the function $U(f_d,f_s)$ still plays the role of a weighting term.

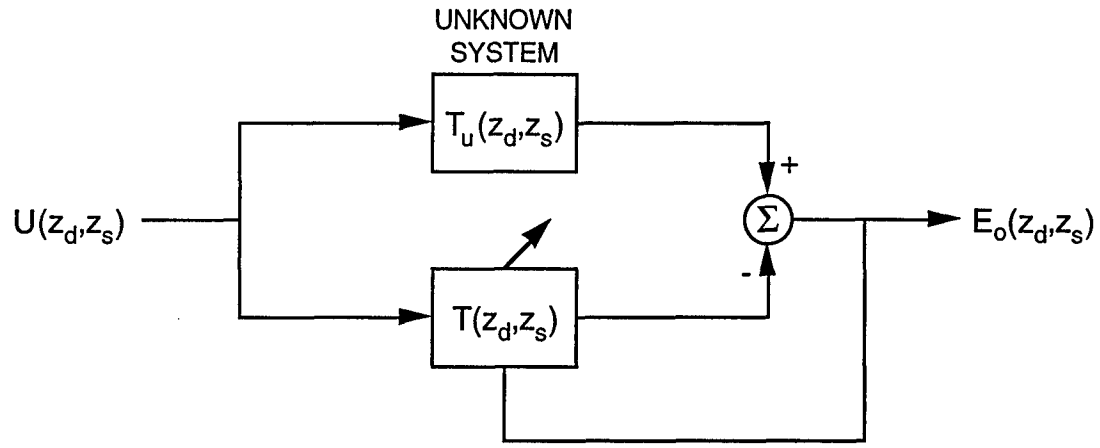


*Figure 3-1. Output error model formulation for 2-D system modeling.*

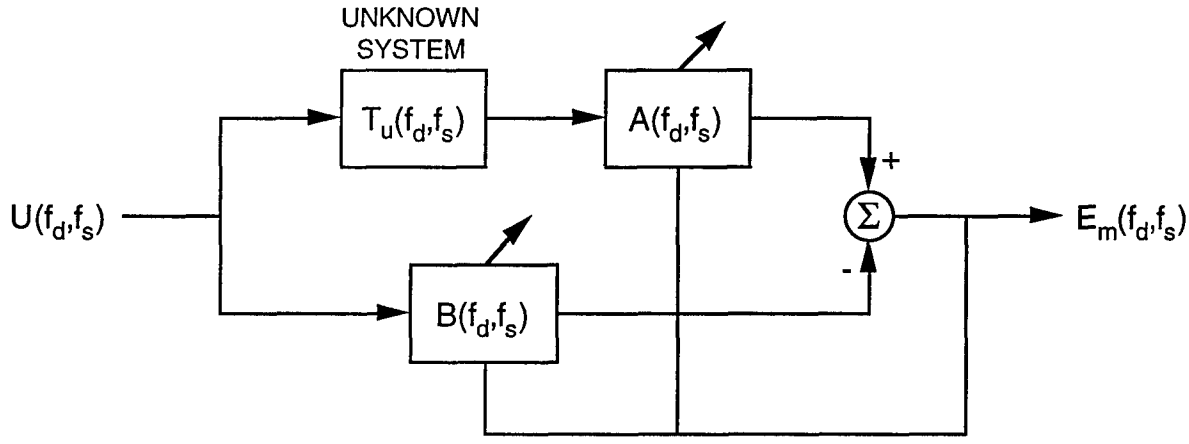


*Figure 3-2. Equation error model formulation for input-driven 2-D system modeling.*

## 3.2 Space-Time Data Modeling Using the 2D-LS-FD Method

In both formulations discussed above (Figures 3-1 and 3-2) the unknown system is available to be driven by the input function $\{u(n,k)\}$, and the input function is known. Neither of these two conditions is true for modeling the space-time phased array radar signal of interest herein. Specifically, in the STAP channel output modeling case only the output of the "unknown system" is available. Here the quotation marks emphasize the fact that the channel output is not the output of a particular ARMA system, but rather, that it is to be approximated as such. In the model matching sense, the channel output sequence is the output of an unknown model with input $\{u(n,k)\}$. If the input is the unit sample sequence, $u(n,k) = \delta(n,k)$, then $\{x(n,k)\}$ can be viewed as the impulse response of the unknown system,

$$X(f_d,f_s) = T_u(f_d,f_s)\, U(f_d,f_s) = T_u(f_d,f_s) \tag{3-4}$$

In Equation (3-4) the second equality is valid because the discrete Fourier transform (DFT) of the unit sample sequence is

$$U(f_d,f_s) = 1 \qquad -0.5 \le f_d \le 0.5; \quad -0.5 \le f_s \le 0.5 \tag{3-5}$$

For this input condition, the equation error is expressed as

$$E(f_d,f_s) = X(f_d,f_s)\, A(f_d,f_s) - B(f_d,f_s) \tag{3-6}$$

This equation error formulation is denoted without subscript in order to emphasize the difference with the previous cases. Notice the similarity in form between the expressions for the equation errors $E_m(f_d,f_s)$ and $E(f_d,f_s)$. A block diagram for the equation error formulation (3-6) is illustrated in Figure 3-3, where the dashed lines represent the condition that the unknown system is unavailable and thus cannot be driven by the input sequence.

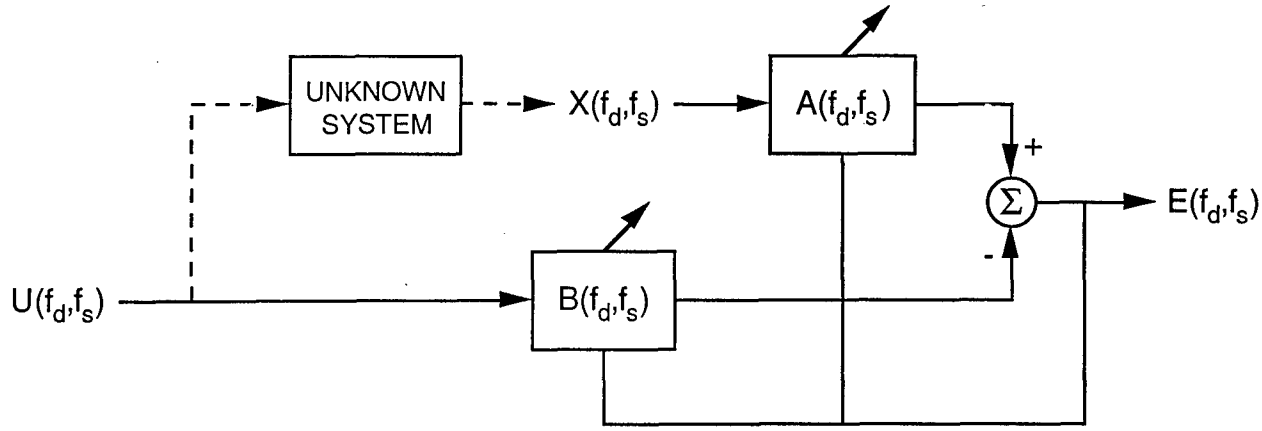


*Figure 3-3. Equation error model formulation for modeling the space-time phased array radar process.*

Minimization of the 2-norm of the equation error $E(f_d,f_s)$ with respect to the unknown ARMA coefficients is a finite-dimensional, linear-space minimization problem. Mikhael and Yu (1994) applied the Orthogonality Theorem to the problem, which leads to a linear set of equations in the unknown parameters $\{a(i_d,i_s)\}$ and $\{b(i_d,i_s)\}$. Such equations have a solution provided the number of equations exceeds the number of unknown parameters. Furthermore, it is necessary to place appropriate constraints in order to avoid the trivial solution, $A(f_d,f_s)=0$ and $B(f_d,f_s)=0$. One such constraint is to set

$$A(f_d,f_s)=1+A_0(f_d,f_s)=1+\sum_{p_d=0}^{P}\sum_{p_s=0}^{P}a(p_d,p_s)\,e^{-j2\pi f_d p_d}\,e^{-j2\pi f_s p_s} \tag{3-7a}$$

$$a(0,0)=0 \tag{3-7b}$$

This constraint is equivalent to the definition of $A(f_d,f_s)$ given in Equations (2-4) and (2-5). Also, notice that the monic feature of

the 2-D polynomial $A(f_d,f_s)$ is retained. Substitution of this constraint into Equation (3-6) results in

$$E(f_d,f_s) = X(f_d,f_s) - [B(f_d,f_s) - X(f_d,f_s)\, A_0(f_d,f_s)] = X(f_d,f_s) - G(f_d,f_s) \tag{3-8}$$

with the 2-D function $G(f_d,f_s)$ defined implicitly as

$$G(f_d,f_s) = B(f_d,f_s) - X(f_d,f_s)\, A_0(f_d,f_s) \tag{3-9}$$

Function $G(f_d,f_s)$ is an auxiliary function introduced to simplify the analysis. Minimizing the 2-norm of the equation error with respect to the unknown coefficients corresponds to minimizing the difference $X(f_d,f_s) - G(f_d,f_s)$. Computational advantages accrue because the problem is formulated in the frequency domain, and the resulting solution is optimal in the least-square sense (Mikhael and Yu, 1994). Once the system model parameters have been identified, the inverse (whitening) system is obtained as the inverse of Equation (2-4), since $T(f_d,f_s)$ is a scalar function.

This method is related to that proposed by Shanks et al. (1972) for the design of 2-D infinite impulse response filters. Shanks' method, however, is formulated in the space-time domain (as opposed to the frequency domain), and its algorithmic implementation is different.

### 3.3 Two-Dimensional MIBDA

In the approach pursued in Phase I, the MIBDA in Figure 2-1 is applicable for 2-D processing also, with the modification that a 2-D ARMA whitening filter is generated for each of the two hypotheses in the MIBDA. However, 2-D convolution in the time domain is a computationally-intensive operation, so an architecture with frequency-domain convolution is preferred. Such an architecture is presented in Figure 3-4 for the case of off-

line filter design. A similar architecture can be defined for the case of on-line filter design. In the architecture of Figure 3-4, the Pre-Processor block can include a variety of operations. Several such functions were identified in Phase I, and evaluated to different degrees of detail. The most important operations for the Pre-Processor block are presented next, in the preferred order of application to the data.

- Spatial nulling of the 1-D vector sequence (this eliminates the effects of barrage-type, point-location jammers, which simplifies the data structure in the frequency domain).
- 1-D vector to 2-D scalar transformation (this is only a conceptual operation since the storage locations of the data remain unchanged).
- Application of a data window (this reduces the effects of sidelobe leakage, at the expense of a loss in resolution, which results in broader spectral features).

In a given configuration, only a subset of these operations may be applied to the data. Optimization of the pre-processing functions will be carried out in the proposed Phase II. This includes analyses such as performance variation as a function of window type applied.

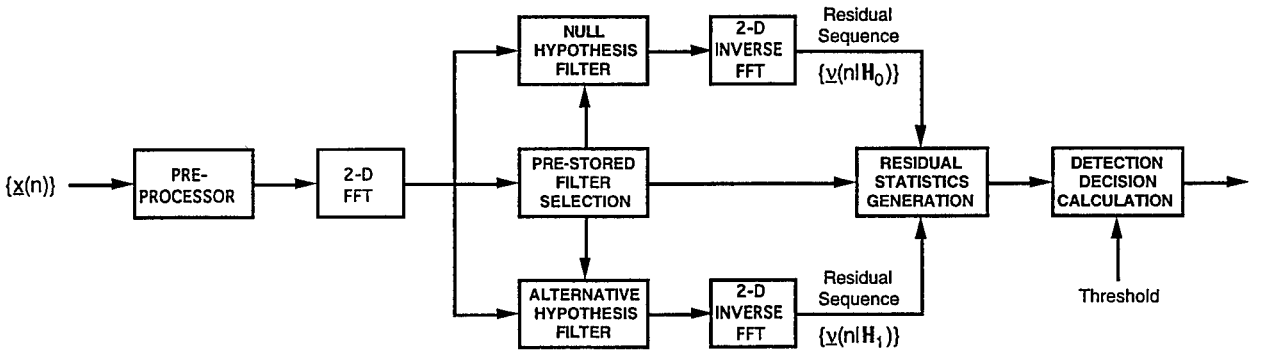


*Figure 3-4. Multichannel innovations-based detector architecture for 2-D data representation.*

The 2-D FFT operation can be followed by an averaging step, which is not shown in Figure 3-4. Averaging the spectral components over several realizations generates a more accurate estimate of the frequency-domain representation. This statement is applicable during hypothesis filter design, as well as in processor architecture design.

It is important to note that, with respect to pre-processing and spectral averaging, the MIBDA design must be compatible with the procedure utilized during hypothesis filter design. For example, if a data window of a specific type is used in the design of the hypothesis filters, then the same data window must be applied in the MIBDA implementation. Likewise, if the hypothesis filters are designed with spectral-domain averaging over $K$ realizations, then the MIBDA must include spectral-domain averaging over $K$ realizations also.

Consider now the 2-D inverse FFT block in Figure 3-4, which includes implicitly the 2-D scalar to 1-D vector transformation. This block is necessary if the hypothesis filter design criteria and/or the detection criteria and decision rules are to be applied in the space-time domain, as opposed to the frequency domain. In a prior program (Román and Davis, 1997) SSC developed a set of hypothesis filter design criteria that are applied in the space-time domain for the 1-D vector MIBDA. Those criteria have been extended in Phase I to the 2-D scalar case, but remain to be implemented in software. Similarly, the likelihood ratio detector used in the 1-D vector MIBDA can be extended to the 2-D scalar case and applied in the space-time domain. Thus, based on the criteria considered thus far, the inverse FFT step is required. However, the alternative of frequency-domain detection is computationally attractive, and will be investigated in the proposed Phase II.

## 3.4 Model Order Determination

Determination of model order is a decision required of all model identification algorithms in applications where the true order of the system generating the channel output data is unknown, or where the process to be modeled is generated by a system which belongs to a different model class. In the second case the model obtained is a "representation model," as opposed to a "physical model" (a model based on accurate analyses of the underlying physical processes). Model order determination is always a difficult problem, and the approaches are often heuristic, at least in part. The approach selected herein is based on the output power (variance) of the model inverse (whitening filter), since the best-fitting model would generate the most whitening (in the sense of whitening the ensemble, not just a particular realization). Such a criterion has to be applied judiciously, however, because it can lead to over-parameterized models since the model with the most possible degrees-of-freedom (number of parameters to be identified) is likely to whiten a specific realization the most. Thus, for a criterion based on the residual power, the model order sought is that value at which the plot of residual power versus model order indicates diminishing returns for further increases in model order (such a value is indicated by a "knee" in the curve).

For a zero-mean 2-D residual sequence of the form in Equation (2-8), the power (variance) is estimated as

$$\hat{\sigma}_v^2 = \frac{1}{JN} \sum_{n=0}^{N-1} \sum_{k=0}^{J-1} |v(n,k)|^2 \tag{3-10}$$

In the context of model order determination adopted herein, the power estimate $\hat{\sigma}_v^2$ is plotted as a function of the order of the

model used to generate the residual sequence, and the model order is selected as the value at which the reduction in residual power is small (in relation to prior reductions) for a unit increase in model order.

A better criterion is one which considers also the effect of the given number of 2-D data points (JN) and the number of parameters being estimated for the model. Akaike (1969; 1970) proposed a simple criterion for AR model order determination referred to as the final prediction error (FPE) which accounts for these two effects. In the FPE criterion the residual power estimate obtained using the Yule-Walker AR parameter estimation algorithm is modified by a multiplicative factor which is a non-decreasing function of the number of data points and the number of parameters being estimated for the model order being evaluated. For a 2-D ARMA($P_d$,$P_s$,$Q_d$,$Q_s$) model and a JxN data matrix, the multiplicative factor corresponding to the one used by Akaike is of the form

$$f(M) = \frac{JN+M}{JN-M} \qquad 0 \le M < JN \tag{3-11}$$

where M is the number of parameters being estimated,

$$M = (P_d + 1)(P_s + 1) + (Q_d + 1)(Q_s + 1) - 1 \tag{3-12}$$

And for the special case where $Q_d = P_d$ and $Q_s = P_s$,

$$M = 2\,(P_d + 1)(P_s + 1) - 1 \tag{3-13}$$

Notice that the function f(M) is non-decreasing. Thus, Akaike's FPE criterion takes into consideration the following two conditions: (a) as the model order increases, the fit of the model to the given data improves (the residual power should decrease

monotonically with increasing model order); and (b) as the model order increases, the fit of the model to an independent realization of the same stochastic process becomes worse on the average (modeling degrees-of-freedom beyond those necessary to model a process are allocated by an identification algorithm to modeling features present only in the realizations used to identify the model).

Akaike's FPE criterion has been the subject of multiple studies, many of which resulted in a modification to the criterion expression. In most cases the FPE has provided a good estimate of the true model order. The extension of the FPE to the 2-D case will be evaluated in the proposed Phase II.

## 4.0 AIRBORNE SURVEILLANCE PHASED ARRAY RADAR APPLICATION

Airborne surveillance for moving target detection using phased array radar systems is one of the major technology thrusts at RL. Consequently, the emphasis devoted to that application in Phase I reflects that significance. The MATLAB software implementation of the 2D-LS-FD algorithm was exercised with simulated multichannel data generated using the SSC-developed software simulation package (Román and Davis, 1997), and selected results are presented herein.

The SSC airborne surveillance phased array radar software model (Vol. II of [Román and Davis, 1997]) is defined for a side-looking, linear, phased array radar configuration, with azimuth scanning capability of ±90 deg from boresight (the effect of multiple elevation channels beamformed into a single channel is included in the model). Each component (target; noise; jammer; clutter) is modeled independently of the others. The structure selected to model each component allows generation of the true covariance matrix sequence, as well as generation of independent statistical data realizations. Moving targets are modeled as point targets in azimuth and elevation, and each moving target is modeled as the output of a first-order linear system in state-space form. This allows for a wide range of conditions (including Swerling Cases 1 through 4 as well as the deterministic case), in a simple and general format. With this structure $G_s$ targets are grouped as a $G_s$th-order linear system. Barrage-type jammers are modeled as point sources of Gaussian-distributed broadband noise in azimuth and elevation. Receiver noise is modeled as uncorrelated in time (pulse-to-pulse) as well as in space (channel-to-channel). Ground clutter is modeled as a large number of statistically-independent clutter patches, with each clutter patch consisting of a large number of individual re-radiators.

Table 4-1 lists the baseline simulation parameter values used to obtain most of the modeling and filtering (whitening) results presented in this section. Clutter-to-noise ratio (CNR) for both sets of the baseline conditions (crab angle values of $\gamma = 0$ deg and $\gamma = 20$ deg) is 47.75 dB. Notice that jammers are not included in these results; this is because the emphasis of the simulation-based analyses has been for ground clutter in receiver noise since it presents the most significant modeling challenge. Also, in one of the alternative configurations jammers are canceled spatially in the pre-processing step. Modeling and whitening runs with jammers present have been made, and the results are similar to those for clutter only. The model structure analysis results shown herein were obtained for parameter values and simulation conditions different from those in the table; the actual parameter values used in such cases are stated clearly. Several cases were run also with the factored form of the classical optimal joint-domain method (Brennan and Reed, 1973), in order to compare the whitening capability of the optimum method with that of the 2D-LS-FD method. Those results show that the 2D-LS-FD method provides significantly more whitening capability than the classical optimal joint-domain method with a limited support size for the sample covariance matrix.

Alternative modeling configurations of the 2D-LS-FD method (ARMA; AR; MA) were evaluated in the context of the airborne surveillance radar array STAP application, with ARMA modeling providing the best model fit and whitening performance. This result is as expected since the ARMA(P,Q) model with $P \geq Q$ provides a larger number of modeling degrees-of-freedom than an AR(P) or an MA(P), with the same dynamic realization requirements. Furthermore, the ARMA(P,Q) model with $P \geq Q$ offers more versatility than an AR(P+Q) or an MA(P+Q). Simulation results also indicate that an ARMA(P,P) model in general provides better modeling than an ARMA(R,Q) with $R < Q$ and $R + Q < 2P$.

| PARAMETER TYPE | PARAMETER (UNITS) | VALUE |
|---|---|---|
| RADAR ARRAY SYSTEM | Number of linear array elements, J | 8 |
| | Number of points in one CPI, N | 64 |
| | Number of elevation axis elements, Je | 4 |
| | Array mainbeam azimuth angle, phi0 (deg) | 30 |
| | Peak transmitted power, Pt (kW) | 200 |
| | Pulse (uncompressed) duration, Tu (μsec) | 200 |
| | Pulse repetition frequency (Hz) | 300 |
| | Radiation frequency, fC (MHz) | 450 |
| | Receiver bandwidth, fB (MHz) | 4 |
| | Transmit pattern gain, Go (dB) | 22 |
| | Receive element gain, Ge (dB) | 4 |
| | Receive element backlobe pattern attenuation, Gb (dB) | -30 |
| | Noise figure, Fn (dB) | 3 |
| | System losses, Ls (dB) | 4 |
| | Transmit pattern array option, patopt | UNIFORM |
| SURVEILLANCE SCENARIO | Platform altitude, Hp (km) | 9 |
| | Platform velocity, Vp (m/sec) | 50 |
| | Range to principal ground clutter ring, rc (km) | 130 |
| | Aircraft platform crab angle, gamma (deg) | 0; 20 |
| TARGET | Narrowband process amplitude, a | 0 |
| | Target radial velocity, Vt (m/sec) | 0 |
| | Target azimuth angle, phit (deg) | 0 |
| | Target elevation angle, thetat (deg) | 0 |
| | Signal-to-noise ratio, SNR (dB) | 0 |
| INTERFERENCE | Jammer azimuth angle, phii (deg) | 0 |
| | Jammer elevation angle, thetai (deg) | 0 |
| | Jammer power, vari | 0 |
| GROUND CLUTTER | Number of ground patches illuminated by mainbeam, Nc | 361 |
| ARRAY NOISE | Receiver noise power per channel, varn | 1 |
| SIMULATION PARAMETERS | Number of realizations used in filter design, Nrd | 20 |
| | Number of realizations used in filter evaluation, Nre | 20 |

*Table 4-1. System parameters and scenario conditions for baseline simulation results.*

## 4.1 Conventional Optimal Joint-Domain Method

Consider the JN-element data vector $\underline{x}_k$ formed by concatenating the N J-element vectors $\{\underline{x}(n)\}$ of the kth range cell in a coherent processing interval (CPI), and let $\hat{\mathcal{R}}$ denote the JNxJN sample covariance matrix estimate obtained by averaging over K independent realizations of the data vector (K range cells, not necessarily contiguous). That is,

$$\hat{\mathcal{R}} = \frac{1}{K}\sum_{k=1}^{K} \underline{x}_k \underline{x}_k^H \tag{4-1}$$

As is well-known, the optimal weight vector is determined as

$$\underline{w}_o = \hat{\mathcal{R}}^{-1}\underline{s} = \left(\hat{\mathcal{R}}^{-1/2}\right)\left(\hat{\mathcal{R}}^{-1/2}\underline{s}\right) \tag{4-2}$$

where $\underline{s}$ is the known, JN-element steering vector. The optimal weight vector is applied to the data in order to generate the detection statistic, $\eta$, as

$$\eta = \underline{w}_o^H \underline{x} = \left(\underline{s}^H \hat{\mathcal{R}}^{-1/2}\right)\left(\hat{\mathcal{R}}^{-1/2}\right)\underline{x} \tag{4-3}$$

Equations (4-2) and (4-3) exhibit the factored form of the optimal joint-domain weight vector: the $\hat{\mathcal{R}}^{-1/2}$ operator is a whitening filter for $\underline{x}$, and the $\underline{s}^H \hat{\mathcal{R}}^{-1/2}$ operator is a matched filter. This factored form is illustrated as a block diagram in Figure 4-1. The intermediate variable in the factored form,

$$\underline{v}_o = \hat{\mathcal{R}}^{-1/2}\underline{x} \tag{4-4}$$

is defined herein as a JN-element residual vector. This residual vector can be transformed into a data array and subsequently into a 2-D scalar sequence, $\{v_o(n,k)\}$, by an association analogous to the

one established in Figure (2-1). Then, the residual optimal conventional 2-D scalar residual sequence can be compared for whiteness with the 2-D scalar residual sequence {v(n,k)} generated by the 2-D whitening filter designed based on the 2D-LS-FD algorithm.

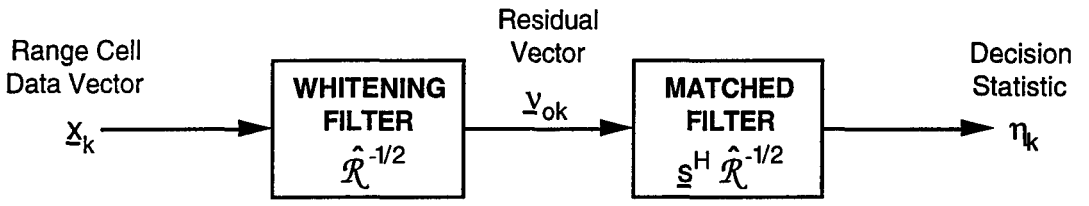


*Figure 4-1. Conventional optimal joint-domain method in factored form.*

The level of whitening can be assessed using the whitening ratio performance measure, which is defined herein as

$$WR = 10 \log_{10}\left[\sum_{n=0}^{N-1}\sum_{k=0}^{J-1}|v(n,k)|^2\right] - 10 \log_{10}\left[\sum_{n=0}^{N-1}\sum_{k=0}^{J-1}|x(n,k)|^2\right] \tag{4-5}$$

This measure can be applied also to a conventional optimal joint-domain residual by substituting $v_o(n,k)$ in place of $v_o(n,k)$.

## 4.2 Simulated Ground Clutter Modeling and Filtering

In the context of time series modeling, selection of the model structure (AR vs. MA vs. ARMA) must be carried out prior to model order determination. However, the two issues are inter-related in a natural manner, and one approach to analyze model structure for a given application is to evaluate the three model types as a function of model order. Such an analysis was carried out in Phase I for the baseline conditions of Table 4-1, with the following alterations: $J = N = 16$; and $N_{rd} = 64$ (number of

realizations used in filter design, which becomes the number of spectra averaged for model identification with the 2D-LS-FD algorithm). Also, $P_d = P_s = P$ and $Q_d = Q_s = Q$ were assumed. Figure 4-2 shows a plot of the 2-D residual power as a function of model order for the $\gamma = 0$ deg case and the following model structures fit to the ground clutter return: (a) an MA(Q) model (dotted line); (b) and AR(P) model (dash-dot line); (c) and ARMA(Q-3,Q) model (dashed line); and (d) and ARMA(P,P) model (solid line). Notice that the ARMA(P,P) model generates the smallest residuals (considering a "smoothed" fit to the curves shown). This result is appealing in the context of MIBDA for the application of interest because the whitening filter associated with an ARMA is also an ARMA.

The results in Figure 4-2 are based on only one generated residual sequence for each plotted point, but similar power values have been obtained with other independent runs. Also, the same conclusion has been obtained with other sets of parameter values. Therefore, the ARMA(P,P) model structure was selected for other analyses, but additional model structure analyses will be made in the proposed Phase II.

Consider now the ARMA(P,P) model structure as a function of model order for the baseline conditions in Table 4-1, including the two crab angle value options ($\gamma = 0$ deg and $\gamma = 20$ deg). Two-dimensional residual power as a function of model order for an ARMA(P,P) model fit to the ground clutter return is presented in Figure 4-3 for both crab angle conditions. Each point of each curve in Figure 4-3 is an average of twenty (20) independent runs, which accounts for the smoother character of these two curves in relation to the curves in Figure 4-2. In Figure 4-3 notice that the minimum residual power is obtained with $P = 6$ for both conditions. Residual power with $P = 6$ is 25.2 dB for $\gamma = 0$ deg, corresponding to a -40.0 dB whitening ratio, and residual power

with $P = 6$ is 24.2 dB for $\gamma = 20$ deg, corresponding to a -41.0 dB whitening ratio. This whitening performance is close to the maximum value attainable, the bound set by the analytical CNR of 47.75 dB.

The parameter values in Table 4-1 were used to generate two sets of whitening performance results, indexed by the two baseline values of crab angle, $\gamma = 0$ deg and $\gamma = 20$ deg. Whitening results (same conditions but different data realizations) were obtained also for the classical optimal joint-domain method in factored form. Those results are discussed next.

A 3-D plot of the channel output power spectrum is presented in Figure 4-4 for the $\gamma = 0$ deg condition. This plot is an average of 20 independent 2-D modified periodograms ("modified" denotes that a data window is applied prior to the FFT). For comparison, the power spectrum of the 2-D ARMA(6,6) model identified from the data is presented in Figure 4-5. Notice the similarity between these two spectral-domain figures.

Figure 4-6 presents a plot of the real part of the 1-D circular ACS of the channel 3 sequence prior to filtering for $\gamma = 0$ deg. This plot is in sharp contrast with Figure 4-7, which is a plot of the real part of the 1-D circular ACS of the channel 3 residual. The filtered sequence is indeed approximately white. Analogously, Figure 4-8 presents a plot of the real part of the 1-D circular ACS of the received signal versus spatial lag ($k$) across the $J = 8$ channels at the time instant corresponding to $n = 16$. And Figure 4-9 presents a plot of the 1-D circular ACS of the real part of the residual across the $J = 8$ channels at the time instant corresponding to $n = 16$. Notice that the unfiltered sequence is highly correlated, whereas the residual is significantly less correlated (it is difficult to assess the level of whiteness for a short-duration sequence). These four figures correspond to $\gamma = 0$

deg conditions. Also, similar results are true for the imaginary part of the respective ACS.

Figures 4-10 and 4-11 present the real part of the circular ACS of the residual as generated by the whitening step of the optimal joint-domain method (see Equation (4-4)) for $\gamma = 0$ deg conditions. These two figures can be compared with Figures 4-7 and 4-9, respectively. For these two figures the sample covariance matrix was generated using $N_{re} = JN = 512$ independent CPI realizations, which is the minimum number of realizations required to obtain a full-rank covariance. This number is 25 times larger than the number of independent realizations ($N_{rd} = N_{re} = 20$) averaged to generate the 2-D frequency-domain representation used to design and to evaluate the ARMA(6,6) model. Clearly, the ARMA-based whitening filter yields residuals with significantly less correlation than the residuals of the optimum joint-domain method.

The whitening ratios calculated for the conventional optimal joint-domain residual are -30.15 dB and -21.96 dB for the $\gamma = 0$ deg and $\gamma = 20$ deg conditions, respectively. These figures are significantly less than those for the 2-D ARMA(6,6) residuals (which are -40.0 dB and -41.0 dB, respectively). This discrepancy is due to the less-than-optimal (although large) number of independent realizations used to generate the JNxJN sample covariance matrix estimate.

Figures 4-12 through 4-19 present the same type of plots as in Figures 4-4 through 4-11, with the following variations. First and foremost, Figures 4-12 through 4-19 were generated for crab angle $\gamma = 20$ deg conditions. Second, channel 4 is selected for the temporal lag plots, instead of channel 3. Third and last, the spatial lag plots are for pulse $n = 44$, instead of $n = 16$. Careful examination of the results presented for $\gamma = 20$ deg conditions re-enforces the observations derived from the earlier figures.

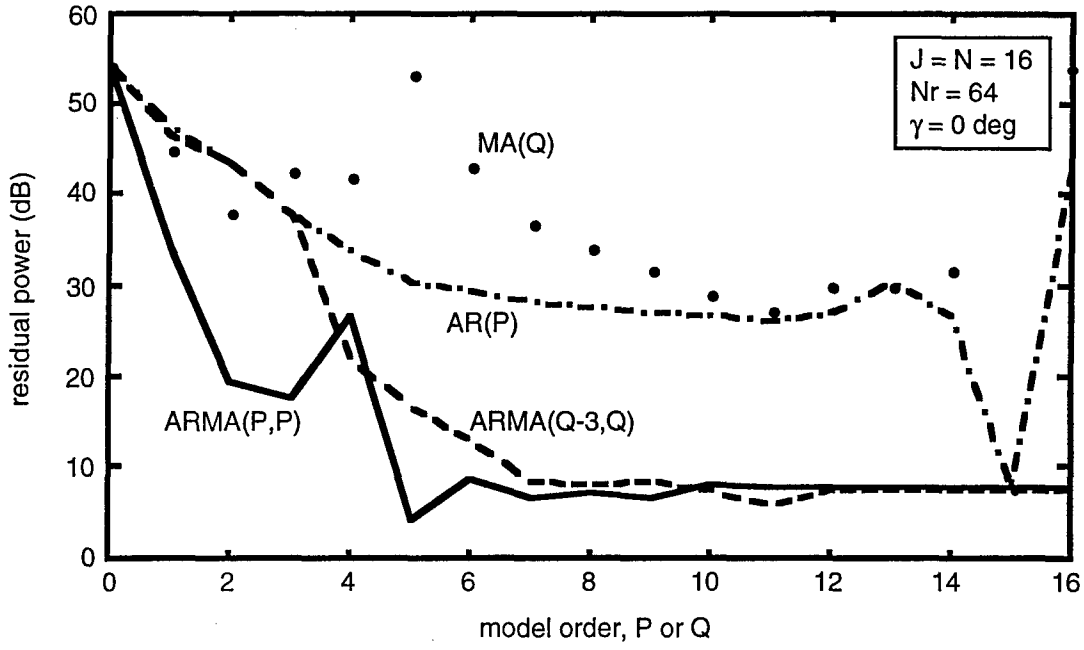


*Figure 4-2. Residual power as a function of model order for 2-D MA, AR, and ARMA models ($J = N = 16$; $N_{rd} = 64$; $\gamma = 0$ deg).*

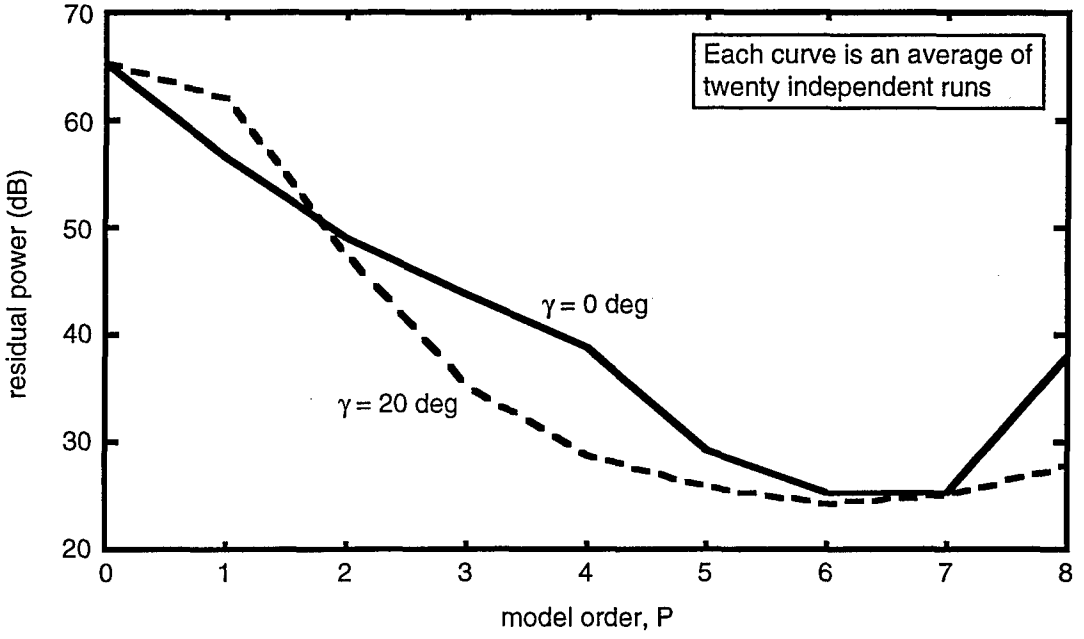


*Figure 4-3. Residual power as a function of model order for a 2-D ARMA(P,P) model for both crab angle conditions.*

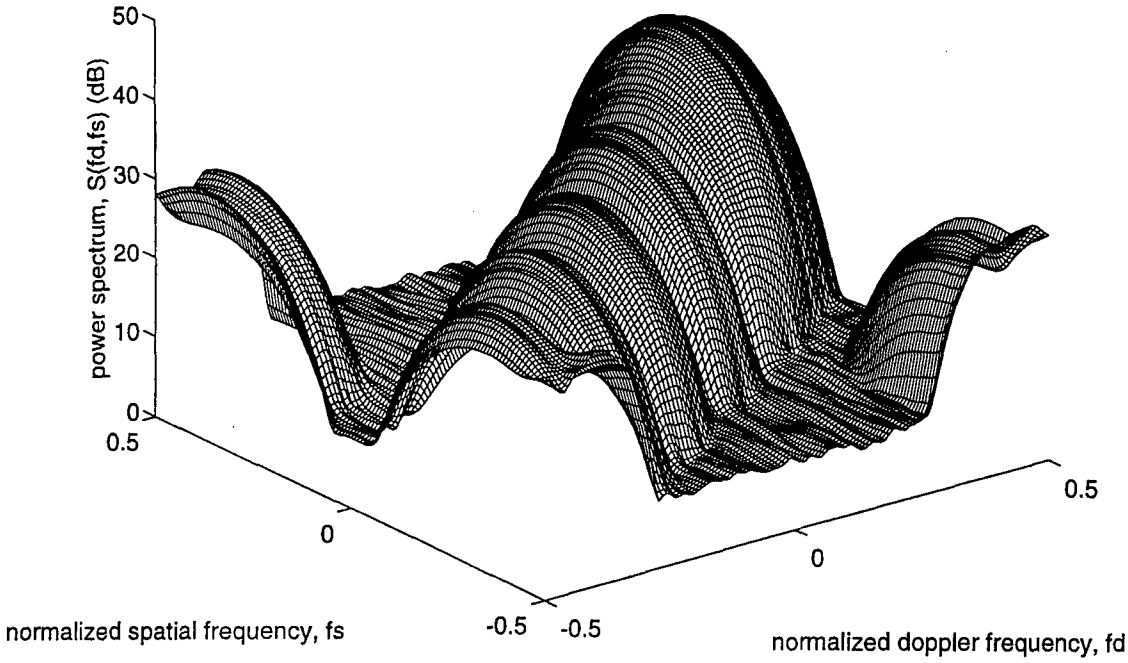


*Figure 4-4. Channel output log power spectrum for $\gamma = 0$ deg.*

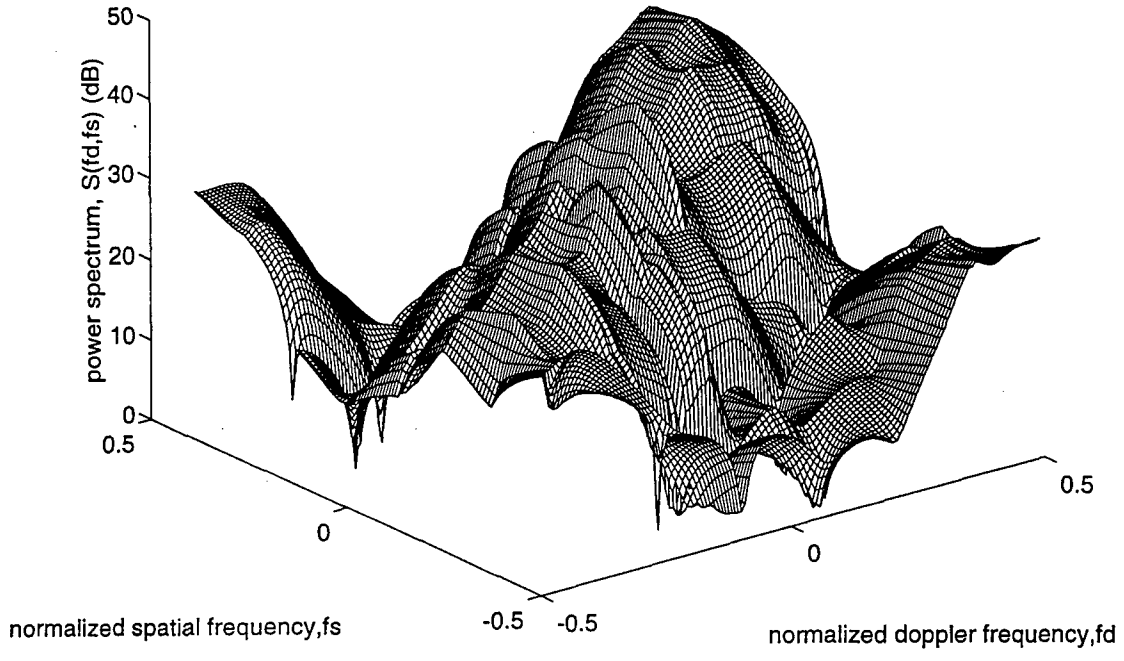


*Figure 4-5. Two-D ARMA(6,6) log power spectrum for $\gamma = 0$ deg.*

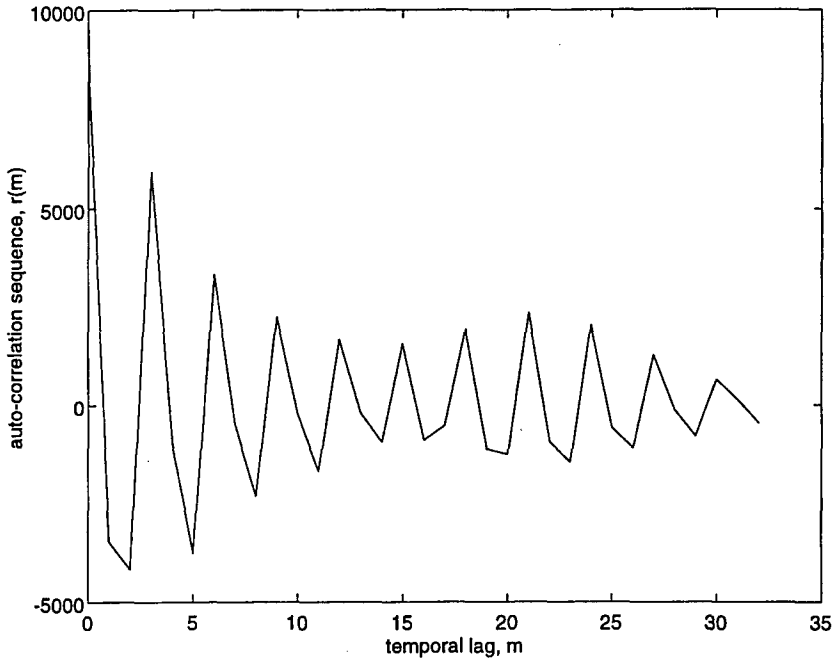


*Figure 4-6. Real part of channel 3 circular ACS versus temporal lag ($\gamma = 0$ deg).*

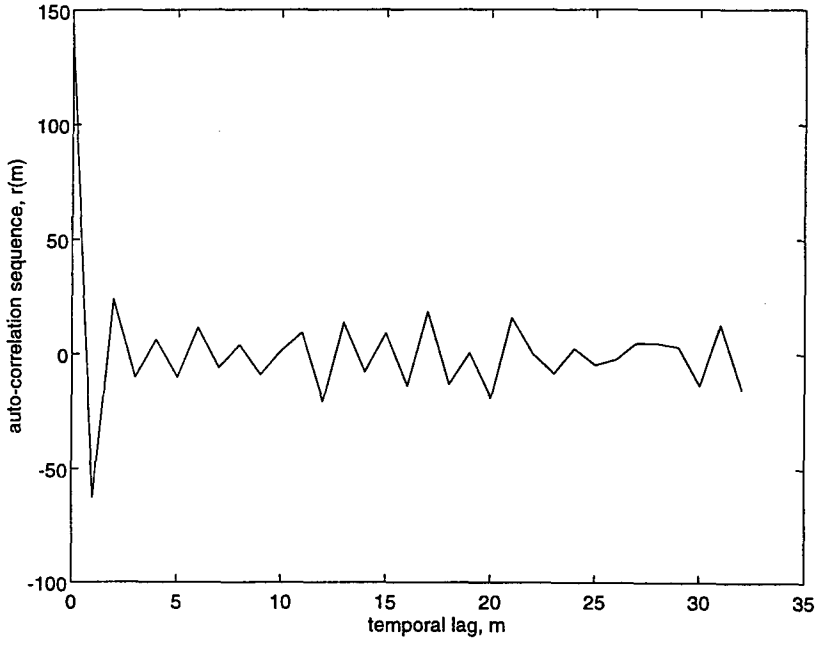


*Figure 4-7. Real part of channel 3 ARMA(6,6) residual circular ACS versus temporal lag ($\gamma = 0$ deg).*

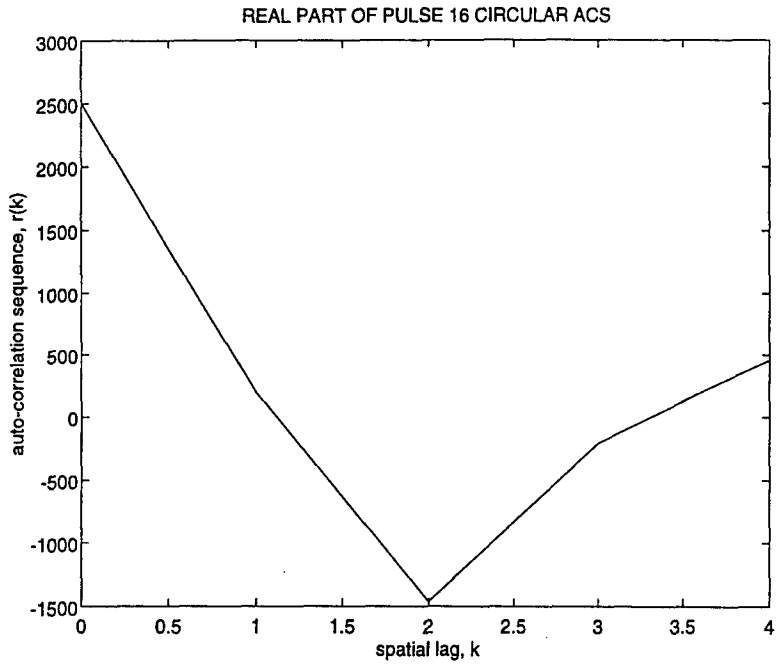


*Figure 4-8. Real part of pulse 16 circular ACS versus spatial lag ($\gamma = 0$ deg).*

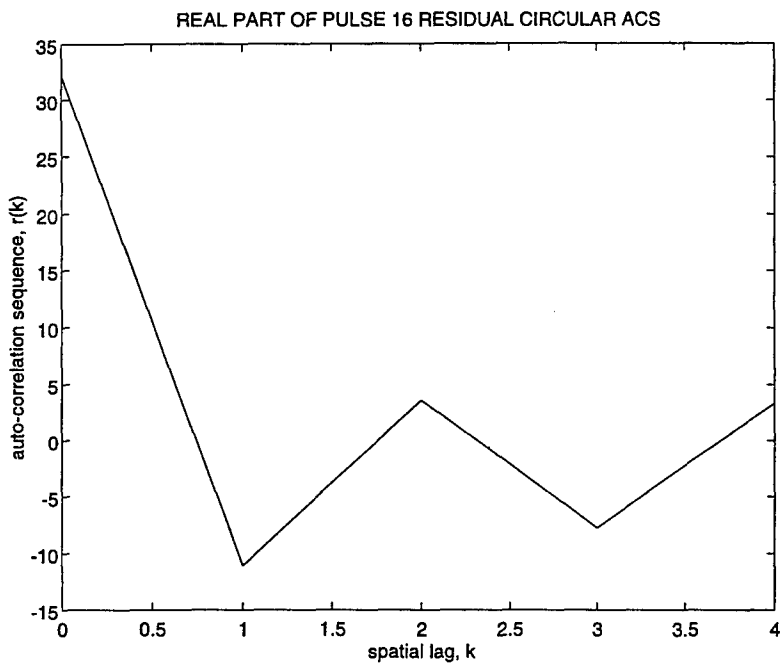


*Figure 4-9. Real part of pulse 16 ARMA(6,6) residual circular ACS versus spatial lag ($\gamma = 0$ deg).*

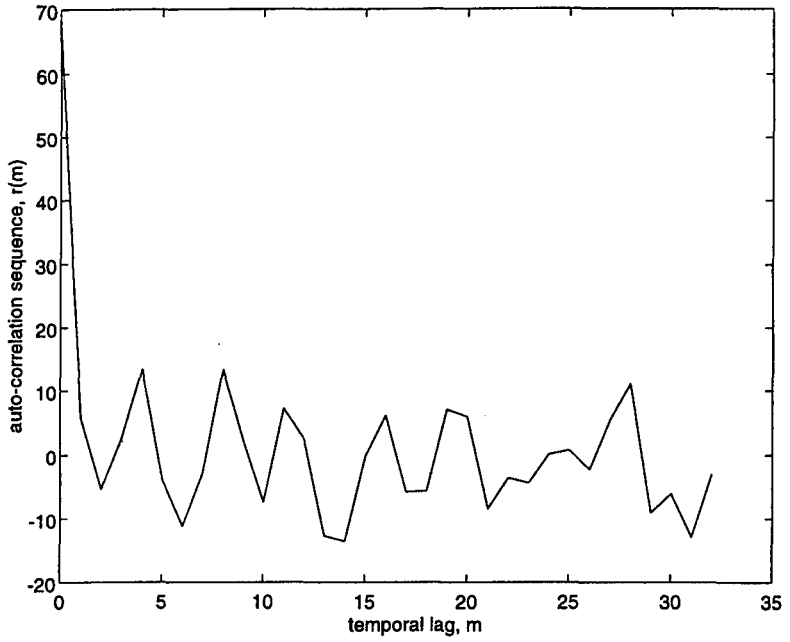


*Figure 4-10. Real part of channel 3 joint-domain residual circular ACS versus temporal lag ($\gamma = 0$ deg).*

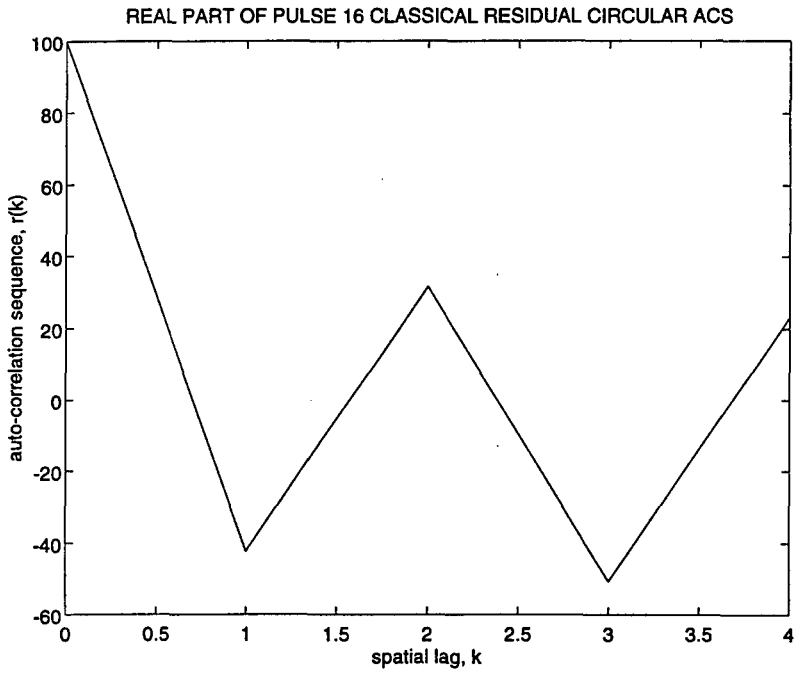


*Figure 4-11. Real part of pulse 16 joint-domain residual circular ACS versus spatial lag ($\gamma = 0$ deg).*

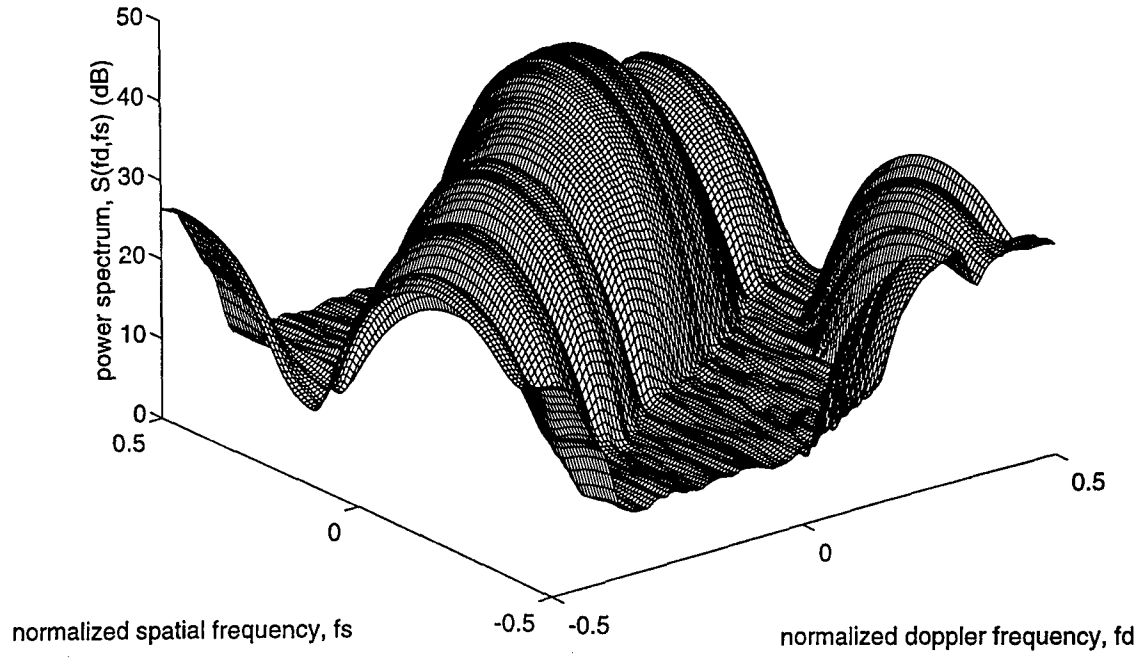


*Figure 4-12. Channel output log power spectrum for $\gamma = 20$ deg.*

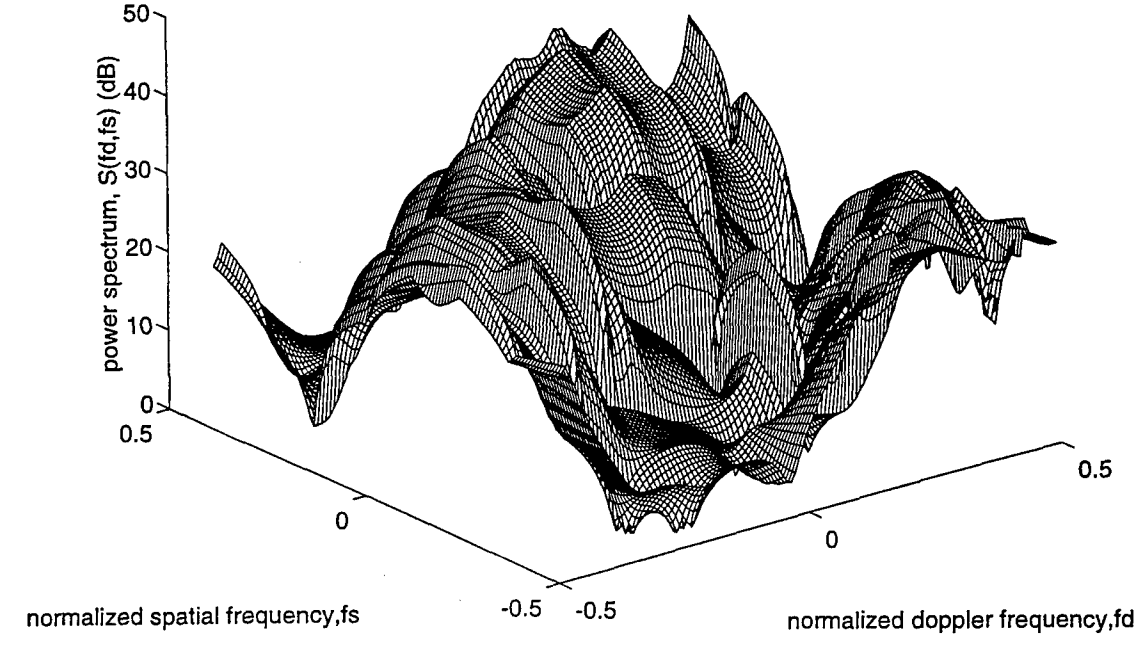


*Figure 4-13. Two-D ARMA(6,6) log power spectrum for $\gamma = 20$ deg.*

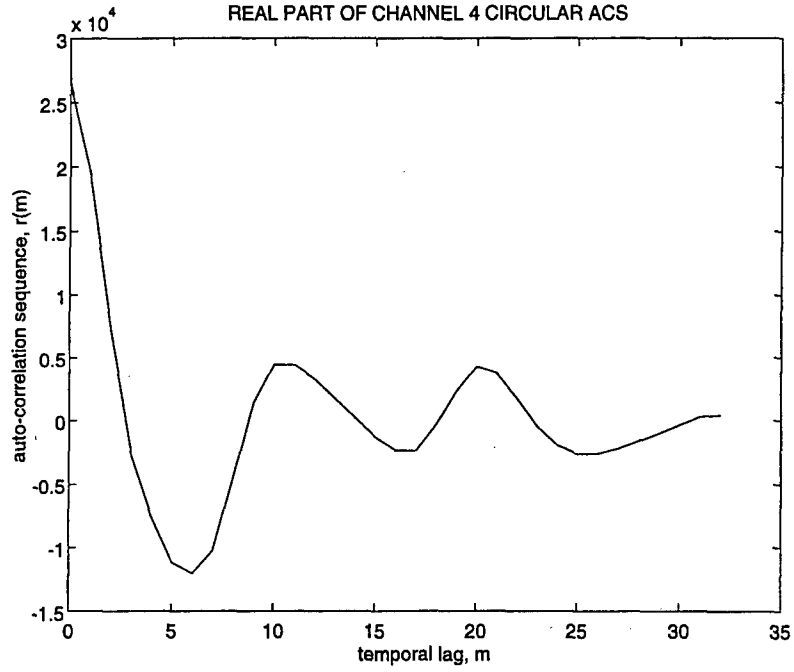


*Figure 4-14. Real part of channel 4 circular ACS versus temporal lag ($\gamma = 20$ deg).*

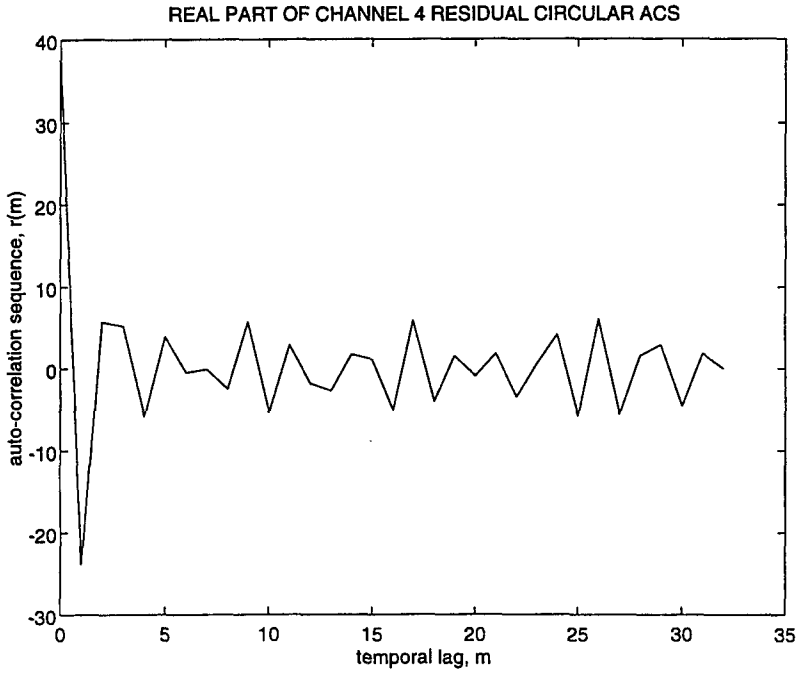


*Figure 4-15. Real part of channel 4 ARMA(6,6) residual circular ACS versus temporal lag ($\gamma = 20$ deg).*

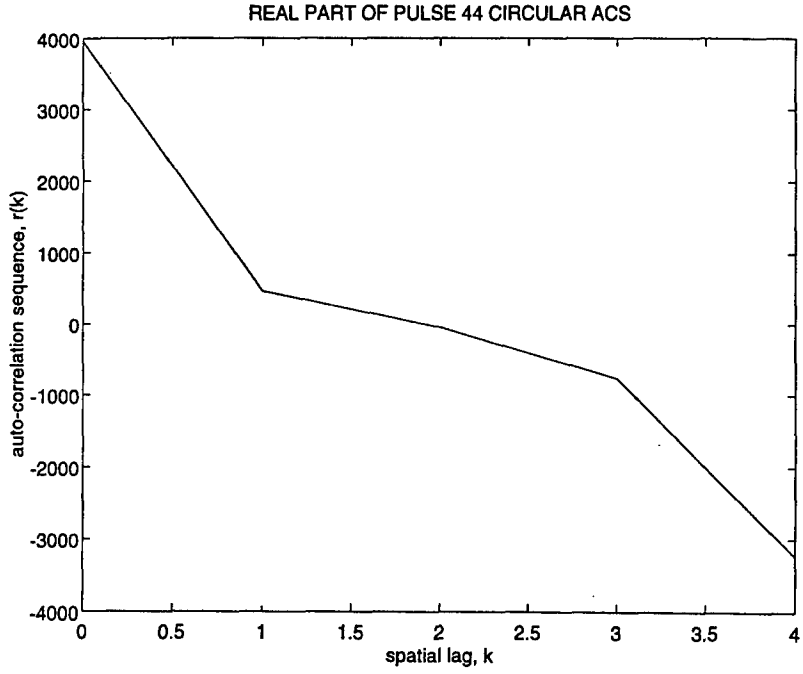


*Figure 4-16. Real part of pulse 44 circular ACS versus spatial lag ($\gamma = 20$ deg).*

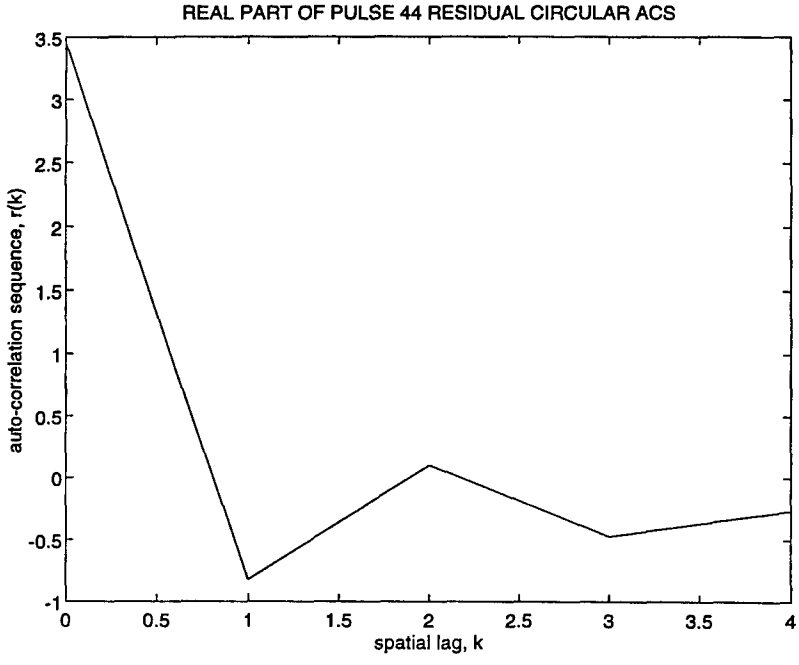


*Figure 4-17. Real part of pulse 44 ARMA(6,6) residual circular ACS versus spatial lag ($\gamma = 20$ deg).*

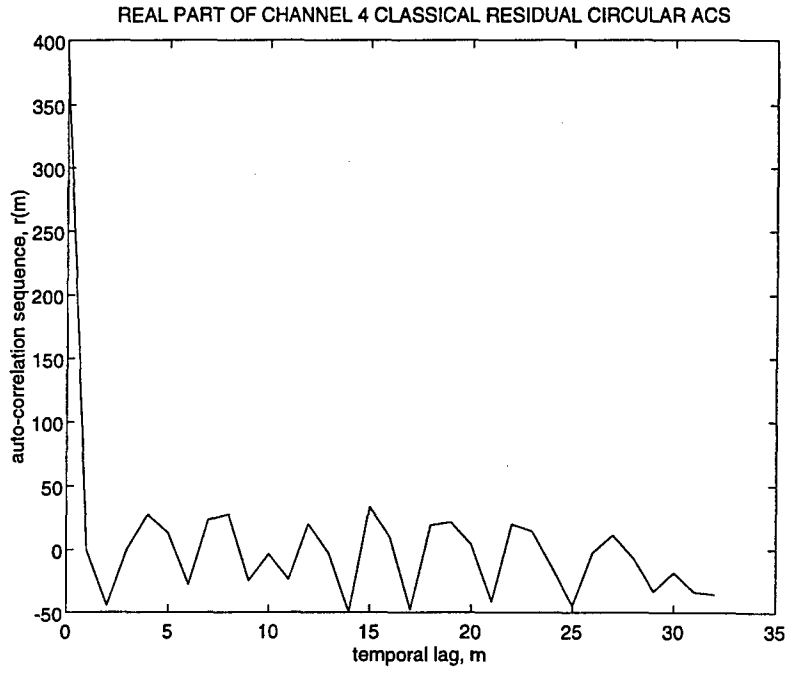


*Figure 4-18. Real part of channel 4 joint-domain residual circular ACS versus temporal lag ($\gamma = 20$ deg).*

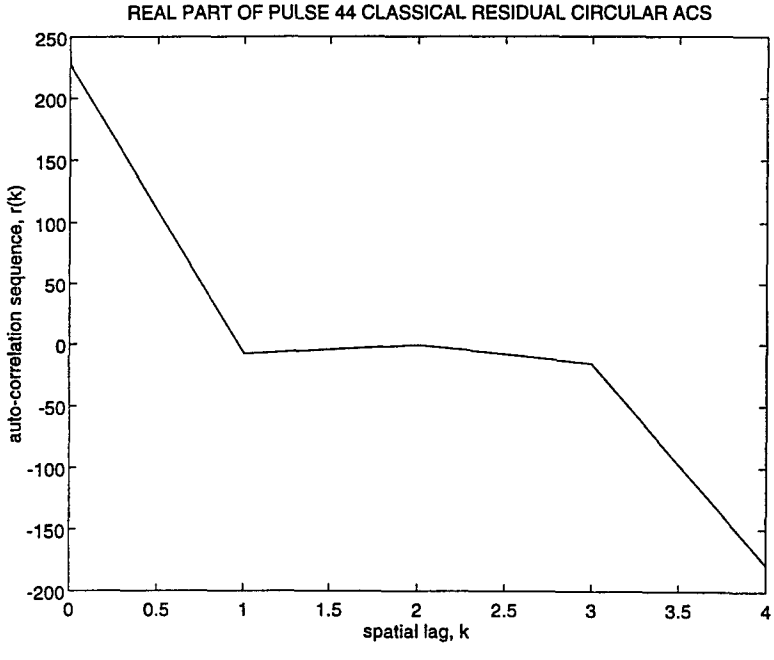


*Figure 4-19. Real part of pulse 44 joint-domain residual circular ACS versus spatial lag ($\gamma = 20$ deg).*

## 5.0 CONCLUSIONS AND RECOMMENDATIONS

In Phase I the STAP problem for airborne surveillance using phased array radar systems was formulated as a 2-D model-based detection problem, and a 2-D innovations-based methodology was formulated. Additionally, a model identification configuration based on the 2D-LS-FD method was developed, and the capability to model the received channel process (with emphasis on the ground clutter process) with a 2-D time series models was established. The 2D-LS-FD method (Mikhael and Yu, 1994) was selected for this study because: (a) model coefficients are identified by solving a linear set of equations; (b) the method is direct (algorithm operates on the data directly, without the need to estimate the ACS); (c) ARMA (rather than just MA or AR) coefficients are generated; (d) the method is simple; and (e) the method is implemented efficiently in software.

A software (MATLAB-based) implementation of the algorithm was developed and exercised using simulated multichannel radar data generated with the SSC-developed software model for phased array radar in an airborne surveillance scenario (Vol. II of [Román and Davis, 1997]). Simulation results obtained in the study validate the modeling capability of the 2D-LS-FD algorithm, and demonstrated favorable performance as a whitening filter in comparison with the conventional optimal joint-domain method using the sample covariance.

In Phase II a MATLAB-based software package will be developed to test STAP algorithms in the context of airborne surveillance radar arrays. This software will include simulated radar data generation, Monte-Carlo analyses capability, and extensive diagnostic functions (for the statistical analysis and dissection of intermediate and final results). Classical and parametric STAP algorithms will be included also. This software will be applied

to evaluate the MIBDA methodology based on 2-D hypothesis filters, and thus establish its performance in relation to classical STAP algorithms and to STAP methods based on various alternative parametric algorithms (Román and Davis, 1993a, 1993b; Michels, 1991). The software will be generated to be compatible with the structure of the Rome Laboratory (RL) STAP (RLSTAP) software analysis and simulation package. This will facilitate integration of the software into RLSTAP at a future date.

The 2D-LS-FD method will be the baseline 2-D algorithm for Phase II due to its attractive features and the performance established in Phase I. Alternative formulations of the method (such as image noise canceling) will be evaluated in the context of the RL airborne surveillance phased array radar application, as well as the to-be-selected dual-use application. Model stability is an important issue for model-based methods in general, and more so in the case of 2-D models. Other candidate algorithms will be implemented in MATLAB-based software, and their performance compared with that of the baseline algorithm.

# APPENDIX A. TWO-DIMENSIONAL REPRESENTATIONS FOR ONE-DIMENSIONAL MULTICHANNEL STATE SPACE MODELS

The analytic representation of the sequence transformation introduced in Section 2.1 (Equation (2-1)) is useful in the understanding of 2-D systems and of the differences/similarities between 1-D and 2-D systems in general. Furthermore, an analytic representation is required to generate the 2-D scalar transfer function and the 2-D scalar power spectrum of a 2-D system related to a 1-D multichannel system. Therrien (1981) presented such a result for the special case of a multichannel AR model, and it is extended herein to cover state space models in innovations representation form. Availability of the 2-D transfer function and power spectrum corresponding to a 1-D multichannel system allows direct comparison of the frequency domain representation of 2-D analytic models of the type presented in Section 2-2 with state variable models (SVMs) of the type employed by Román and Davis (1993a; 1993b) in other model-based MIBDA work.

## A.1 Transformation of a One-Dimensional Vector Sequence Into a Two-Dimensional Scalar Sequence

Consider the 1-D multichannel to 2-D scalar association in Equation (2-1), repeated herein for convenience:

$$x_{J-k}(n) = x(n,k) \qquad 0 \le n \le N-1;\ 0 \le k \le J-1 \tag{A-1}$$

Recall that Equation (A-1) assumes channel $J$ is the temporal and spatial reference for the array. For an equally-spaced linear array with array spacing $d$, the signal at channel $k$ is a delayed (or advanced) version of the signal at channel $k-1$. With channel $J$ as the temporal and spatial reference, it follows that

$$\text{(A-2a)} \qquad \underline{x}(n) = \begin{bmatrix} x_1(n) \\ \vdots \\ x_{J-1}(n) \\ x_J(n) \end{bmatrix} = \begin{bmatrix} e^{-j2\pi f_s \kappa} x_J(n) \\ \vdots \\ e^{-j2\pi f_s} x_J(n) \\ x_J(n) \end{bmatrix} = x_J(n) \begin{bmatrix} e^{-j2\pi f_s \kappa} \\ \vdots \\ e^{-j2\pi f_s} \\ 1 \end{bmatrix} \qquad 0 \le n \le N\text{-}1$$

$$\text{(A-2b)} \qquad \underline{x}(n) = e^{-j2\pi f_s \kappa} x_J(n) \begin{bmatrix} 1 \\ e^{j2\pi f_s} \\ \vdots \\ e^{j2\pi f_s \kappa} \end{bmatrix} = x_1(n) \underline{e}_J(f_s) \qquad 0 \le n \le N\text{-}1$$

$$\text{(A-2c)} \qquad \kappa = J - 1$$

where $f_s$ is the normalized spatial frequency corresponding to an azimuth angle $\phi$ and an elevation angle $\theta$ (both $\phi$ and $\theta$ are defined with respect to the array boresight for a side-looking array), and is defined as

$$\text{(A-3)} \qquad f_s = \frac{d}{\lambda_C} \cos(\theta) \sin(\phi)$$

where $\lambda_C$ is the narrowband radiation wavelength. Element k of $\underline{e}_J(f_s)$ is the operator representing k-1 spatial advances. Vector $\underline{e}_J(f_s)$ is referred to as the spatial frequency vector at frequency $f_s$, and can be expressed in terms of the spatial Z-transform variable restricted to the unit circle as

$$\text{(A-4)} \qquad \underline{e}_J(f_s) = \begin{bmatrix} 1 \\ e^{j2\pi f_s} \\ \vdots \\ e^{j2\pi f_s \kappa} \end{bmatrix} = \begin{bmatrix} z_s^0 \\ z_s^1 \\ \vdots \\ z_s^\kappa \end{bmatrix}$$

$$\text{(A-5)} \qquad z_s = e^{j2\pi f_s}$$

Consequently, the spatial frequency vector can be denoted also as $\underline{e}_J(z_s)$. This alternative notation is more appropriate for analyses involving transfer functions. From Equations (A-1) and (A-2), the association between a 1-D multichannel vector sequence and a 2-D scalar sequence is defined as

(A-6) $$\underline{x}(n) = x_1(n)\underline{e}_J(f_s) \iff \{x(n,k) \mid k = 0,1,\ldots,J-1\}$$

In Relation (A-6) the subscript "1" is dropped from the 2-D sequence, for simplicity.

## A.2 Innovations Representation State Variable Model

The innovations representation of the channel output process $\{\underline{x}(n)\}$ is a linear, shift-invariant, stochastic SVM of the form

(A-7a) $$\underline{\alpha}(n+1) = F\underline{\alpha}(n) + K\underline{\varepsilon}(n) \qquad n \geq 0$$

(A-7b) $$\underline{x}(n) = H^H\underline{\alpha}(n) + \underline{\varepsilon}(n) \qquad n \geq 0$$

(A-7c) $$\underline{\alpha}(0) = \underline{0}$$

(A-7d) $$E[\underline{\alpha}(n)\underline{\alpha}^H(n)] = \Pi(n) = \Pi \qquad n \neq 0$$

where $F$ is the $n_s x n_s$ system matrix, $K$ is the $n_s x J$ input distribution matrix, and $H$ is the $n_s x J$ observation matrix. In this model, $\underline{\alpha}(n)$ is the $n_s$-element state vector, $\underline{x}(n)$ is the J-element output vector, and $\{\underline{\varepsilon}(n)\}$ is a zero-mean, white, Gaussian, J-element vector sequence with correlation matrix structure given as

(A-8) $$E[\underline{\varepsilon}(n)\underline{\varepsilon}^H(n-m)] = \Omega\,\delta(m) \qquad \forall\, n, m$$

(A-9) $$\delta(m) = \begin{cases} 1 & m = 0 \\ 0 & m \neq 0 \end{cases}$$

The sequence $\{\underline{\varepsilon}(n)\}$ is referred to as the innovations, and matrix $K$ in Equation (A-7a) is the Kalman gain. An innovations representation SVM has several properties and characteristics that simplify model identification and other problems (Anderson and Moore, 1979; Román and Davis, 1993b).

Consider now an instantaneous, linear transformation on the innovations sequence based on the LDU decomposition of the innovations covariance matrix, $\Omega$. That is,

(A-10) $$\underline{v}(n) = T^H \underline{\varepsilon}(n)$$

(A-11) $$T^H = D^{-1/2} L^{-1}$$

(A-12) $$\Omega = L D L^H = (T^{-1})^H T^{-1}$$

In the LDU decomposition of Equation (A-12) the JxJ matrix $D$ is diagonal and real-valued, and the JxJ matrix $L$ is lower-triangular with 1's along the main diagonal. The covariance matrix of the transformed innovations sequence is the identity matrix,

(A-13) $$E[\underline{v}(n)\underline{v}^H(n-m)] = I\,\delta(m) \qquad \forall\, n, m$$

This transformed innovations is both spatially and temporally uncorrelated (Therrien, 1981). In this new basis for the input sequence, SVM (A-7) becomes

(A-14a) $$\underline{\alpha}(n+1) = F\underline{\alpha}(n) + KC\,\underline{v}(n) \qquad n \geq 0$$

(A-14b) $$\underline{x}(n) = H^H\underline{\alpha}(n) + C\,\underline{v}(n) \qquad n \geq 0$$

where the JxJ matrix $C$, introduced herein for notational simplicity, is defined as

(A-15) $$C = (T^H)^{-1} = (T^{-1})^H = L D^{1/2}$$

It is important to note that this alternative SVM representation is equivalent to SVM (A-7) from an input-output perspective, but SVM (A-14) is not an innovations representation. SVM (A-14) with $\{\underline{v}(n)\}$ uncorrelated and normalized as in Equation (A-13) is referred to herein as a generalized innovations representation.

The JxJ transfer function matrix of the SVM (A-14) is denoted herein as $T_{GI}(z_d)$, where $z_d$ is the temporal (Doppler) z-transform variable restricted to the unit circle,

(A-16) $$z_d = e^{j2\pi f_d}$$

and $f_d$ is the normalized Doppler frequency shift. In terms of the model parameters, $T_{GI}(z_d)$ is given as

(A-17) $$T_{GI}(z_d) = T_{IR}(z_d)\, C = [\, H^H (z_d I - F)^{-1} K + I \,] C = H^H (z_d I - F)^{-1} KC + C$$

where $T_{IR}(z_d)$ is the transfer function matrix of the innovations representation, SVM (A-7). SVM (A-14) is introduced herein to simplify the generation of 2-D frequency-domain representations for multichannel SVMs, as shown in Section A-4.

The square matrix factor $(z_d I - F)^{-1}$ in $T_{IR}(z_d)$ contributes the multivariable poles of the SVM. Specifically, the determinant of matrix $(z_d I - F)$ is a polynomial in the variable $z_d$ whose roots are the multivariable system poles. In contrast, all the matrices in the transfer function expression contribute to the value of the multivariable system zeros (the multivariable zero definition preferred herein is that of Davison and Wang [1974, 1976]). The dynamic behavior (in the temporal domain) of the SVM is determined by the multivariable system poles and zeros jointly.

## A.3 Whitening Filter State Variable Model

An important feature of the innovations representation is that SVM (A-7) is causal and causally-invertible. As such, the inverse system is obtained directly from SVM (A-7). Specifically, the inverse system for SVM (A-7) is

(A-18a) $$\underline{\alpha}(n+1) = [F - KH^H]\,\underline{\alpha}(n) + K\underline{\varepsilon}(n) = A\underline{\alpha}(n) + K\underline{x}(n) \qquad n \geq 0$$

(A-18b) $$\underline{\varepsilon}(n) = -H^H\underline{\alpha}(n) + \underline{x}(n) \qquad n \geq 0$$

(A-18c) $$\underline{\alpha}(0) = \underline{0}$$

(A-18d) $$E[\underline{\alpha}(n)\underline{\alpha}^H(n)] = \Pi(n) = \Pi \qquad n \neq 0$$

where all vectors and matrices are defined previously except the $n_s x n_s$ matrix $A$, which is defined implicitly as

(A-19) $$A = F - KH^H$$

Notice that the input to this SVM is the channel output sequence, and the output is the temporally-uncorrelated sequence $\{\underline{\varepsilon}(n)\}$. Thus, SVM (A-18) is the whitening filter corresponding to SVM (A-7). An important relation between SVM (A-7) and its inverse SVM (A-18) is that the multivariable system poles and zeros of SVM (A-7) are the multivariable system zeros and poles, respectively, of SVM (A-18). Also, SVM (A-18) is an innovations representation (the inverse system of an innovations representation is itself an innovations representation).

Consider again the spatially-whitening instantaneous, linear transformation applied to the innovations sequence, Equation (A-10). Application of this transformation to the output equation of

the whitening filter leads to the following generalized whitening filter,

(A-20a) $$\underline{\alpha}(n+1) = [F - KH^H]\,\underline{\alpha}(n) + K\underline{\varepsilon}(n) = A\underline{\alpha}(n) + K\underline{x}(n) \qquad n \geq 0$$

(A-20b) $$\underline{v}(n) = -T^H H^H \underline{\alpha}(n) + T^H \underline{x}(n) \qquad n \geq 0$$

As before, the innovations representation property is lost by the introduction of the linear transformation on $\underline{\varepsilon}(n)$.

The JxJ transfer function matrix of the SVM (A-20) is denoted herein as $T_{GW}(z_d)$, where $z_d$ is the temporal (Doppler) z-transform variable defined previously, Equation (A-16). In terms of the model parameters, $T_{GW}(z_d)$ is given as

(A-21) $$T_{GW}(z_d) = T^H T_{WF}(z_d) = T^H[-H^H(z_d I - A)^{-1}K + I] = -T^H H^H (z_d I - A)^{-1}K + T^H$$

where $T_{WF}(z_d)$ is the transfer function of the whitening filter, SVM (A-18).

## A.4 Two-Dimensional Frequency-Domain Representations of a Multichannel State Variable Model

Two-dimensional frequency-domain representations are derived next for each of two SVMs: the generalized innovations representation (A-14), and the generalized whitening filter (A-20). Consider first the generalized innovations representation case. The input to the generalized innovations representation is the generalized innovations sequence $\{\underline{v}(n)\}$. A relation analogous to (A-6) can be established also for the generalized innovations; namely,

(A-22) $$\underline{v}(n) = v_1(n)\,\underline{e}_J(f_s) \quad \Longleftrightarrow \quad \{v(n,k) \mid k = 0, 1, \ldots, J-1\}$$

Now let $X(z_d,z_s)$ and $N(z_d,z_s)$ denote the 2-D Z-transform of $\{x(n,k)\}$ and $\{v(n,k)\}$, respectively. Given these definitions and the form of SVM (A-14), the scalar 2-D transfer function $T_{GI}(z_d,z_s)$ of the 1-D multichannel system (A-14) is obtained as

$$X(z_d,z_s) = T_{GI}(z_d,z_s)\, N(z_d,z_s) \tag{A-23}$$

$$T_{GI}(z_d,z_s) = \frac{1}{J}\, \underline{e}_J^H(z_s)\, T_{GI}(z_d)\, \underline{e}_J(z_s) = \frac{1}{J}\, \underline{e}_J^H(z_s)\, T_{IR}(z_d)\, C\, \underline{e}_J(z_s) \tag{A-24}$$

Figure A-1 is a block diagram representation for these relations. The factor $J^{-1}$ in Equation (A-24) is required to preserve the power between the input and output. Consider the case where $T_{GI}(z_d)$ is the identity matrix. In such a case it follows that $\{x(n,k)\} = \{v(n,k)\}$, provided the factor $J^{-1}$ is included (since $\underline{e}_J^H(z_s)\, \underline{e}_J(z_s) = J$). It is possible to view this factor in a different way. Specifically, the spatial frequency vector can be defined to be of unit norm, which requires normalization of the right side of Equation (A-4) by a factor of the form $J^{-1/2}$.

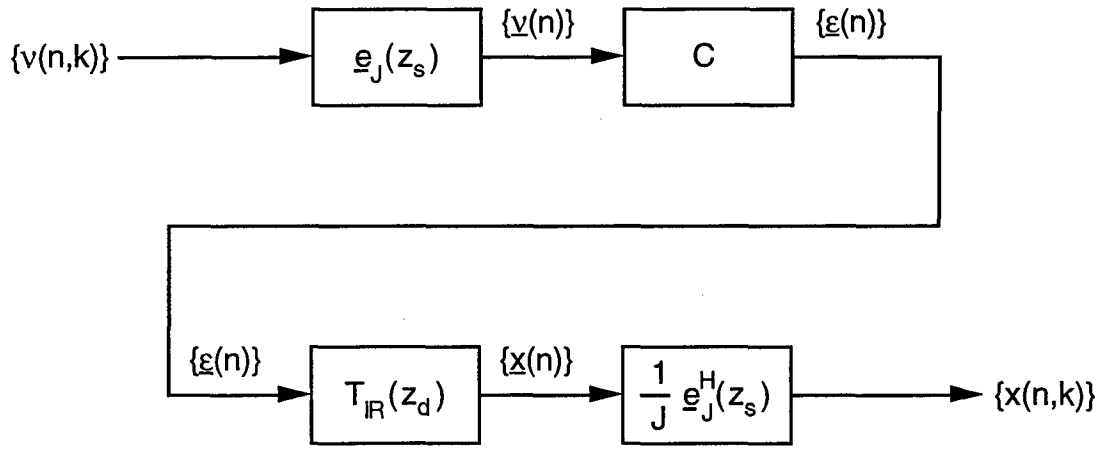


*Figure A-1. Block diagram for the 2-D scalar transfer function of a 2-D system related to a 1-D multichannel system in generalized innovations representation form.*

The temporal frequency content of the 2-D transfer function $T_{GI}(z_d,z_s)$ is determined by the temporal dynamics (multivariable poles and zeros) of the generalized innovations transfer function, $T_{GI}(z_d)$. In turn, the spatial frequency content of the 2-D transfer function is determined by the spatial frequency vector $\underline{e}_J(z_s)$, which inherently models a delay, but does not include spatial dynamics. This condition may limit the capability of 1-D vector models to represent scenarios where the coupling between channels is partial (where the noise-free output of a given channel is not a delayed or advanced replica of the noise-free output of the adjacent channels). Such scenarios include cases where the crab angle is non-zero and/or where the clutter ridge slope is different from unity. Further analysis of the modeling capability of 1-D vector SVM's is required to assess this issue, and will be carried out in the proposed Phase II.

The 2-D power spectrum of the linear, shift-invariant system in Figure A-1 is the square of the magnitude of the scalar transfer function evaluated at the unit circle in the complex plane (with $f_d$ and $f_s$ replacing $z_d$ and $z_s$ in order to represent this fact); that is,

$$S_{GI}(f_d,f_s) = T_{GI}(f_d,f_s)\,T^*_{GI}(f_d,f_s) = \left|T_{GI}(f_d,f_s)\right|^2 \tag{A-25}$$

$$-0.5 \le f_d \le 0.5 \quad \text{and} \quad -0.5 \le f_s \le 0.5$$

And the power spectrum of the 2-D channel output sequence, denoted herein as $S_{xx}(f_d,f_s)$, is determined as (Anderson and Moore, 1979)

$$S_{xx}(f_d,f_s) = S_{GI}(f_d,f_s)\,S_{vv}(f_d,f_s) = \left|T_{GI}(f_d,f_s)\right|^2 S_{vv}(f_d,f_s) \tag{A-26}$$

$$-0.5 \le f_d \le 0.5 \quad \text{and} \quad -0.5 \le f_s \le 0.5$$

where $S_{vv}(f_d,f_s)$ is the power spectrum of the 2-D generalized innovations sequence, $\{v(n,k)\}$. Since $\{\underline{v}(n)\}$ is temporally and spatially white (Equation (A-13)), it follows that

(A-27) $$E[v(n,k)v^*(n-m,k-\ell)] = \delta(m,\ell) \qquad \forall\, n, m, k, \ell$$

(A-28) $$\delta(m,\ell) = \begin{cases} 1 & m=0 \text{ and } \ell=0 \\ 0 & m\neq 0 \text{ or } \ell\neq 0 \end{cases}$$

(A-29) $$S_{vv}(f_d,f_s) = 1 \qquad \forall\, f_d, f_s$$

Then Equation (A-26) becomes

(A-30) $$S_{xx}(f_d,f_s) = S_{GI}(f_d,f_s) = \left|T_{GI}(f_d,f_s)\right|^2$$

$$-0.5 \le f_d \le 0.5 \quad \text{and} \quad -0.5 \le f_s \le 0.5$$

which is the desired frequency-domain representation for the generalized innovations SVM.

Consider now the generalized whitening filter case. The input to the generalized whitening filter is the channel output sequence, and the output is the generalized innovations sequence. Based on Relations (A-6) and (A-22) and on the form of SVM (A-20), the scalar 2-D transfer function $T_{GW}(z_d,z_s)$ of the multichannel generalized whitening filter is obtained as

(A-31) $$N(z_d,z_s) = T_{GW}(z_d,z_s)\, X(z_d,z_s)$$

(A-32) $$T_{GW}(z_d,z_s) = \frac{1}{J}\, \underline{e}_J^H(z_s)\, T_{GW}(z_d)\, \underline{e}_J(z_s) = \frac{1}{J}\, \underline{e}_J^H(z_s)\, T^H\, T_{WF}(z_d)\, \underline{e}_J(z_s)$$

with $T_{GW}(z_d)$ as defined in Equation (A-21). Transfer function $T_{GW}(z_d,z_s)$ is presented in block diagram form in Figure A-2.

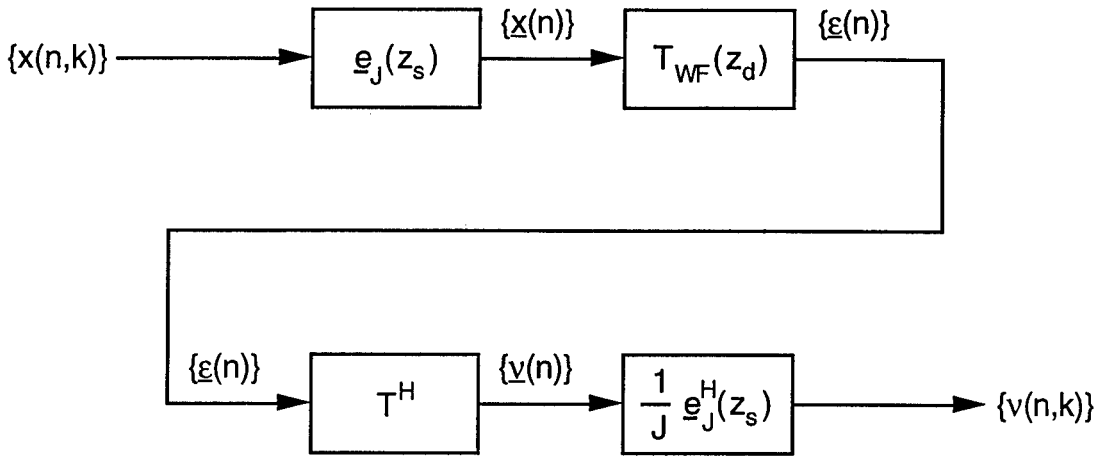


*Figure A-2. Block diagram for the 2-D scalar transfer function of a 2-D system related to a 1-D multichannel system in generalized whitening filter form.*

The 2-D power spectrum of the linear, shift-invariant system in Figure A-2 is the square of the magnitude of the scalar transfer function evaluated at the unit circle in the complex plane (with $f_d$ and $f_s$ replacing $z_d$ and $z_s$ in order to represent this fact); that is,

$$S_{GW}(f_d,f_s) = T_{GW}(f_d,f_s)T^*_{GW}(f_d,f_s) = \left|T_{GW}(f_d,f_s)\right|^2 \qquad \text{(A-33)}$$

$$-0.5 \le f_d \le 0.5 \quad \text{and} \quad -0.5 \le f_s \le 0.5$$

Equation (A-33) is the desired frequency-domain representation for the generalized whitening filter SVM. And the power spectrum of the 2-D generalized innovations sequence is determined as (Anderson and Moore, 1979)

(A-34) $$S_{vv}(f_d,f_s) = S_{GW}(f_d,f_s)\, S_{xx}(f_d,f_s) = \left|T_{GW}(f_d,f_s)\right|^2 S_{xx}(f_d,f_s)$$

$$-0.5 \le f_d \le 0.5 \quad \text{and} \quad -0.5 \le f_s \le 0.5$$

with $S_{vv}(f_d,f_s)$, the power spectrum of the 2-D generalized innovations sequence, of the form in Equation (A-29).

## REFERENCES


H. Akaike

(1969) "Fitting Autoregressive Models for Prediction," Annals of the Institute of Statistical Mathematics, Vol. 21, pp. 243-247.

(1970) "Statistical Predictor Identification," Annals of the Institute of Statistical Mathematics, Vol. 22, pp. 203-217.

B. D. O. Anderson and J. B. Moore

(1979) Optimal Filtering, Prentice-Hall, Englewood Cliffs, NJ.

L. E. Brennan and I. S. Reed

(1973) "Theory of adaptive radar," IEEE Transactions on Aerospace and Electronic Systems, Vol. AES-9, No. 2 (March), pp. 237-252.

E. J. Davison and S. H. Wang

(1974) "Properties and calculation of transmission zeros of linear multivariable systems," Automatica, Vol. 10, pp. 643-658.

(1976) "Remark on multiple transmission zeros of a system," Automatica, Vol. 12, p. 195.

D. E. Dudgeon and R. M. Mersereau

(1984) Multidimensional Digital Signal Processing, Prentice-Hall, Englewood Cliffs, NJ.

A. G. Jaffer, M. H. Baker, W. P. Ballance, and R. J. Staub

(1991) Adaptive Space-Time Processing Techniques for Airborne Radar, RL Technical Report No. RL-TR-91-162, Rome Laboratory, Rome, NY.

S. L. Marple, Jr.
(1987) Digital Spectral Analysis With Applications, Prentice-Hall, Englewood Cliffs, NJ.

P. A. S. Metford and S. Haykin
(1985) "Experimental analysis of an innovations-based detection algorithm for surveillance radar," IEE Proceedings, Vol. 132, Pt. F, No. 1 (February), pp. 18-26.

J. H. Michels
(1991) Multichannel Detection Using the Discrete-Time Model-Based Innovations Approach, Rome Laboratory Technical Report No. RL-TR-91-269, Rome Laboratory, Rome, NY.

W. B. Mikhael and H. Yu
(1994) "A linear approach for two-dimensional, frequency domain least square signal and system modeling," IEEE Transactions on Circuits and Systems - II: Analog and Digital Signal Processing, Vol. 41, No. 12 (December), pp. 786-795.

M. Rangaswamy and J. H. Michels
(1997) "A parametric multichannel detection algorithm for correlated and non-Gaussian random processes," Proceedings of the IEEE National Radar Conference (NATRAD '97), Syracuse, NY, May 13-15.

J. R. Román and D. W. Davis
(1993a) Multichannel System Identification and Detection Using Output Data Techniques, Rome Laboratory Technical Report No. RL-TR-93-141, Rome Laboratory, Rome, NY.
(1993b) State-Space Models for Multichannel Detection, Rome Laboratory Technical Report No. RL-TR-93-146, Rome Laboratory, Rome, NY.

(1997) Multichannel System Identification and Detection Using Output Data Techniques - Phase II, Rome Laboratory Technical Report No. RL-TR-97-5, Vols. I and II, Rome Laboratory, Rome, NY.

J. L. Shanks, S. Treitel, and J. H. Justice

(1972) "Stability and Synthesis of Two-Dimensional Recursive Filters," IEEE Transactions on Audio and Electroacoustics, Vol. AU-20, No. 2 (June), pp. 115-128.

C. W. Therrien

(1981) "Relations Between 2-D and Multichannel Linear Prediction," IEEE Transactions on Acoustics, Speech, and Signal Processing, Vol. ASSP-29, No. 3 (June), pp. 454-456.

(1986) The Analysis of Multichannel Two-Dimensional Random Signals, Naval Postgraduate School Technical Report No. NPS62-87-002, Naval Postgraduate School, Monterey, CA.

J. Ward

(1994) Space-Time Adaptive Processing for Airborne Radar, Technical Report No. TR-1015 (December), contract no. F19628-95-C-0002, Lincoln Laboratory, Massachusetts Institute of Technology, Lexington, MA.

☆U.S. GOVERNMENT PRINTING OFFICE: 1998-610-130-61095

# *MISSION OF ROME LABORATORY*

Mission. The mission of Rome Laboratory is to advance the science and technologies of command, control, communications and intelligence and to transition them into systems to meet customer needs. To achieve this, Rome Lab:

a. Conducts vigorous research, development and test programs in all applicable technologies;

b. Transitions technology to current and future systems to improve operational capability, readiness, and supportability;

c. Provides a full range of technical support to Air Force Material Command product centers and other Air Force organizations;

d. Promotes transfer of technology to the private sector;

e. Maintains leading edge technological expertise in the areas of surveillance, communications, command and control, intelligence, reliability science, electro-magnetic technology, photonics, signal processing, and computational science.

The thrust areas of technical competence include: Surveillance, Communications, Command and Control, Intelligence, Signal Processing, Computer Science and Technology, Electromagnetic Technology, Photonics and Reliability Sciences.

**DEPARTMENT OF THE AIR FORCE**
**AIR FORCE RESEARCH LABORATORY (AFMC)**

15 Jun 04

MEMORANDUM FOR DTIC-OCQ
ATTN: Larry Downing
Ft. Belvoir, VA 22060-6218

FROM: AFRL/IFOIP

SUBJECT: Distribution Statement Change

1. The following documents (previously limited by SBIR data rights) have been reviewed and have been approved for Public Release; Distribution Unlimited:

ADB226867, "Multichannel System Identification and Detection Using Output Data Techniques", RL-TR-97-5, Vol 1.

ADB176689, "Multichannel System Identification and Detection Using Output Data Techniques", RL-TR-93-141.

ADB198116, "Multichannel Detection Using Higher Order Statistics", RL-TR-95-11.

ADB232680, "Two-Dimensional Processing for Radar Systems", RL-TR-97-127.

ADB276328, "Two-Dimensional Processing for Radar Systems", AFRL-SN-RS-TR-2001-244.

2. Please contact the undersigned should you have any questions regarding this memorandum. Thank you very much for your time and attention to this matter.

KELLY CAGWIN
STINFO Officer
Information Directorate
315-330-7094/DSN 587-7094